Introductory Fracture Mechanics

Lecture Notes

by - George R. Irwin

110 pages

Ideas and Events of Historical Interest

During the 1920's, statistical methods had sufficiently developed so as to provide certain simplifications applicable to "extreme value" situations. These were suitable for elementary forms of nucleation theory applicable, for example, to the growth of raindrops in a cloud of water vapor. [redacted] Polyani at the Berlin Hochschule encouraged and suggested ideas of that type. The result was to focus attention upon certain irregularities which possessed significant growth or motion possibilities. Thus, Orowan, whose doctoral thesis at the Berlin Hochschule (1930) was devoted to the crystalline dislocation idea in application to yielding of metals, recalls that he was asked [redacted] in his doctoral examination to give a procedure for estimating the tensile strength of a pure liquid. From ideas under discussion at that time, the procedure went as follows.

Assume a spherical hole of volume, ω, occurs inside of a liquid subjected to a tension, σ. Assume the piston producing the tension moves slowly, the container walls are rigid, and ω is small compared to the expansion, Δ, necessary to produce the tensile stress. The total system energy, U_T, neglecting heat, consists ~~in~~ of the stress field energy plus the surface tension energy of the hole. Thus

$$U_T = \frac{1}{2}\ \sigma(\Delta-\omega) + \gamma A \qquad (1)$$

where γ is the surface energy (per unit area) and A is the surface area of the spherical hole. Variations of the hole size are assumed to occur rapidly compared to motion of the piston.

Thus, with the container volume essentially fixed, the system has a maximum potential energy condition of unstable equilibrium relative to variations of ω when

$$\frac{dU_T}{d\omega} = \frac{1}{2}(A-\omega)\frac{d\sigma}{d\omega} - \frac{1}{2}\sigma + \gamma\frac{dA}{d\omega} = 0 \qquad (2)$$

The fractional change of σ with change of ω is given by

$$\frac{d\sigma}{\sigma} = -\frac{d\omega}{A-\omega} \qquad (3)$$

Thus equation (2) becomes

$$\frac{dU_T}{d\omega} = \gamma\frac{dA}{d\omega} - \sigma = 0 \qquad (4)$$

or

$$\frac{\sigma r}{2} = \gamma \qquad (5)$$

where r is the radius of the spherical hole. In response to the examination question, Orowan pointed out that the liquid tensile strength could be calculated in terms of γ and equation (5) by choice of a suitable value for r. This, in turn, was supplied by assuming that, since liquid molecules are mobile, holes of the approximate size of a single molecule must not be infrequent. Thus, an estimate of the liquid tensile strength (expected to be moderately high) was given by

$$\sigma = \frac{4\gamma}{D} \qquad (6)$$

where D is the molecular diameter.

A similar basic idea was used by A. A. Griffith (1920) in formulating a theory of fracture strength for brittle materials. Griffith assumed such materials would contain small cracks and that unstable extension of the largest of these would determine the fracture strength. As in the case of the liquid illustration, the total system energy would be maximum and

in unstable equilibrium relative to the crack size when the rate of release of stress field energy was just balanced by the rate of increase of surface energy.

Griffith's estimate of the rate of release of stress field energy (now termed $\mathcal{G}$) was derived from a two-dimensional analysis of stresses around an elliptical opening in a large plate published by Inglis (1913). In equation form, the Griffith theory of crack strength had the form

$$\mathcal{G} = \frac{\sigma^2 \pi a}{E} = 2\gamma \qquad \frac{\sigma^2 \pi a}{E} \qquad (7)$$

where σ is the remote tensile stress normal to the crack, a is the half-length of the two-dimensional crack, E is Young's Modulus, and γ is the solid state surface energy.

A smaller degree of success would be expected for the basic idea in application to solids than in application to liquids. Nevertheless, experimental trials with glass gave encouraging results. It is now known that experiments with "dry" glass would have provided crack strength results corresponding to a surface energy of about 7,000 ergs/cm^2. However, "dry" testing conditions require special effort. In addition, his experiments with thin bulbs of glass using internal pressure may have been influenced by local bulging of the region containing the initial crack. In any case, Griffith's experimental results were interpreted as corresponding to values of γ not far from 1000 ergs/cm^2 which seemed like a fair value for the surface energy at that time.

Although the Griffith crack theory was accepted as basic by those studying the strength of glass, this viewpoint was slow to receive interest among those primarily concerned with structural metals. Careful investigations were made of the energy which must be exerted to fracture notched steel bars

of various size by Stanton and Batson (1920) and by Docherty (1935). Despite exact attention to dimensional similitude in terms of notch root radius and specimen geometry, both investigations showed that a large decrease occurred in the fracture work per unit specimen volume with increase of specimen size. Although these results were disturbing with regard to applicability of structural model testing, they did not directly suggest applicability of the Griffith crack theory because the work rate found was not proportional to fracture area. The result found was intermediate between proportionality to specimen volume and proportionality to fracture area.

In a widely read 1941 review paper, Goerge Sachs stated that plastic flow behaviors can be analyzed assuming dimensional similitude whereas, in the case of fracture, an increase in degree of brittleness occurs with increase of dimensions. No explanations other than experimental facts were given by Sachs. His observation had an influence upon investigations of fracture brittleness of armor for naval vessels conducted at the University of North Carolina during World War II. In a summary of that work by Shearin and others (1948), the fracture work results for notched bars were divided into the work prior to cracking of the notch root and the "post-cracking" work. In line in Sach's comment, it was found that the "precrack" work was nearly proportional to specimen volume (in scaled experiments). Most of the "size-effect" pertained to the energy required to move the leading edge of an already formed crack.

In the development of a post World War II fracture program at the U. S. Naval Research Laboratory, it was decided to attempt establishment of a relationship between the work rate to move an already formed crack and the

stress field energy release rate. It was recognized this work rate would consist in plastic strains near the crack and would not be appreciably influenced by the solid state surface energy of the material. The initial paper (by Irwin) discussing this viewpoint is in the ASM Symposium volume "Fracturing of Metals" (1948) as is the above paper by Shearin et al. The correspondence of the new viewpoint to the Griffith crack theory was pointed out. It was, in fact, suggested that an equation similar to equation (7) might pertain to onset of rapid crack extension with a plastic-work-dependent constant substituted in place of 2γ. By 1952, a wide applicability of this idea was apparent. Furthermore, the fact that relationships similar to the modified form of Equation (7) would supply connections between design stress and allowable flaw size was considered of special importance. The discussions of the modified Griffith theory by Irwin and Kies in two Welding Journal papers, 1952 and 1954, reflected a degree of optimism with regard to practical applicability which was shared by very few fracture scholars at that time.

Orowan independently published the plastic work rate modification of the Griffith crack theory in 1949 and 1952. In Orowan's view, the idea was primarily of interest for research guidance. Irwin and Kies claimed the modified Griffith theory could be used for practical estimates of fracture strength so long as fracture occurred in advance of general yielding. A wide divergence of opinions on fracture strength existed prior to 1960 which could be resolved only by refinement and development of fracture mechanics technology. However, the degree of acceptance of fracture-mechanics, evident during 1960, was enough to guarantee continued growth of the subject. This acceptance arose primarily from the intensive study devoted to three major fracture problems during the period 1954-1960.

In the first of these, failure of the de Havilland "Comet" commercial jet aircraft, the official report was disappointing, in the sense that reference was made only to fatigue and inadequate window reinforcement as the factors responsible. However, the importance of crack propagation in the "Comet" failures was clearly acknowledged by the use of materials of greater crack-toughness and by the introduction of crack-arrest design features in subsequent commercial jet planes. The fracture safety of any aircraft structure rests primarily on the ability of components to resist propagation of such cracks as may, unavoidably, develop during service before replacement. The average stress level in the pressure hull of the "Comet" was about one-third of the yield strength of the material. Because of inadequate window reinforcement, the effective crack size determining the driving force for crack propagation was less than necessary the size of the window where fatigue cracking occurred.

In the period 1954-1956, a series of incidents occurred involving large steam turbine electric current generators in which heavy (100,000 lb) steel rotating components fractured unexpectedly during service use. The serious dangers, in terms of damage and of financial loss, stimulated a very intensive study of the problem. The laboratory tests most closely simulating the service failures were those in which rotational speed was employed to fracture large notched discs. A satisfactory correlation of these tests with other fracture tests, applying the available concepts of fracture mechanics, was provided by Wundt and his associates at General Electric (Schenectady). These same concepts assisted understanding of the service failures. In agreement with the laboratory fracture tests, examination of the service fractures

suggested that the starting cracks had grown to a size of the order of several inches before the development of rapid crack propagation. Local concentrations of impurities were usually associated with these cracks and the stable growth possibilities were enhanced by the presence of hydrogen. The average stress on the region containing the primary origin was 30% of the yield strength.

This fracture problem stimulated interest in ultrasonic inspection and a demand for steel components of greater toughness and cleanness. The desired degree of improvement of the steel was achieved mainly through the enhanced soundness of the forgings made possible by better steel-melting practice and by the installation of vacuum-pouring equipment during 1957-1959. In addition the steel composition was improved so as to provide a significant increase in the fracture toughness of the metal.

The third major fracture problem was concerned with steel solid-propellant rocket chambers. This resulted in extensive investigations of crack propagation in very high-strength metals, beginning in 1958. Careful examinations of fracture failure coupled with realistic methods of laboratory crack-toughness evaluation, again proved most useful. The rocket chambers which experienced serious cracking troubles were fabricated by welding and heat-treated, after welding, to a yield strength in the range 190,000-215,000 lb/in^2. Fabrication cracks were always involved in these failures. With rare exceptions these occurred in welds or along weld borders. Large improvements in the accuracy of inspection, assisted by smooth finishing of the welds and the elimination of moisture-induced stress-corrosion, were necessary. When the crack-toughness of the material was maintained at a sufficiently high level so that a small crack half through the cylindrical

wall section was stable with the normal tension equal to the yield stress, it was possible to effect the welding and inspection with enough care for reliable production chambers to be obtained.

In 1959, the American Society for Testing Materials established a special committee for fracture testing of high-strength metals. The First Report of this committee (January, 1960) stated that "the validity of the analytical methods of fracture mechanics is sufficiently well established" to permit their use in determining whether a fracturetest "is measuring the significant quantities governing performance" and the degree in which a fracture-test result "may be generalized to the more complex structure existing in service". The A.S.T.M. committee* provided tentative recommendations on crack-toughness measurement procedures which have been extensively applied.

* now termed ASTM E-24

REFERENCES

1. A. A. Griffith, Phil. Trans. Roy. Soc., 1920, Vol. A 221, p. 163.
2. W. Weibull, Ing. Veteuskaps Akad. Handlinger, 1939, p. 151.
3. T. E. Stanton and R. G. C. Batson, Proc. Inst. Civil Eng., 1921, Vol. 211, p. 211.
4. J. G. Docherty, Engineering, 1932, Vol. 133, p. 645, also 1935, Vol. 139, p. 211.
5. G. Sachs, Trans. Amer. Inst. Min. Met. Eng., 1941, Vol. 143, p. 13.
6. G. E. Inglis, Trans. Inst. Naval Architects, 1913, Vol. 55, p. 219.
7. ASM Symposium Volume, "Fracturing of Metals", Cleveland, 1948 (see Chapters by G. R. Irwin and by P. Shearin et al).
8. E. Orowan, Rep. Progress Physics, 1949, Vol. 12, p. 185.

The Crack Extension Force, $\mathcal{G}$, from Energy Principles

In mechanics, forces are sometimes derived from energy considerations. Assume there is a block of mass, m, resting on an inclined plane which makes an angle, θ, with the horizontal, and that the contact friction is large enough so that the block is stationary. In order to find the force, f_s, on the block tending to cause sliding, we could resolve the total force of gravity, mg, into components normal to the plane and parallel to the expected direction of sliding. Alternatively we can imagine an increment of sliding displacement of the block, ds. Then the force, f_s, is given by the equation

$$f_s\, ds = mg\, ds \sin\theta \qquad (1)$$

where the right side of equation (1) is the loss of potential energy from the system corresponding to the imagined or "virtual" displacement, ds, of the block. The result, $f_s = mg \sin\theta$, is the same as would have been obtained by resolving the total force of gravity on the block into vector components. However, the energy method using a virtual displacement is more general and can be used to define a generalized force in a situation where the tendency of the force to cause forward motion of a process cannot be visualized in a simple way.

In order to establish studies of progressive fracturing in terms of quantitative characterization and observation, it is necessary to define the force tending to cause crack extension. This can be done with a maximum degree of simplicity if we assume that the system (test plate or component) containing the crack has only one energy reservoir, the elastic stress field, and that increments of forward motion of the process can be taken as increments, dA, of new separational area. From the principles of theoretical mechanics

it then follows that the crack-extension-force, $\mathcal{G}$, is given by

$$\mathcal{G} = - \frac{dU_T}{dA} \quad \text{(system isolated)} \qquad (2)$$

where U_T is the total stress field energy. The "system isolated" requirement simply means that, if no energy enters or leaves the plate at the loading points during the crack extension, dA, the loss of stress field energy, $-dU_T$, can be directly associated with the increment of crack extension, dA.

The system isolated requirement can be removed if the energy entering the stress field through motion of the loading forces is taken into account. For example, suppose a test plate of thickness, B, contains a through-crack of length, a, as shown in Figure 1.* Assume the specimen is pin-loaded (as shown) and that the increase in separation of the loading points due to application of a load, P, is Δ. If the load-displacement changes by $d\Delta$ during the increment of crack extension, $dA = B\,da$, then dU_T is augmented by an amount $P\,d\Delta$ which represents energy which is stored and recoverable. The net change of stress field energy representing the energy loss associated with crack extension is therefore dU_T minus $P\,d\Delta$. Thus the equation for $\mathcal{G}$ becomes

$$\mathcal{G}\,(B\,da) = - (dU_T - P\,d\Delta)$$
$$= P\,d\Delta - dU_T \qquad (3)$$

It was assumed above that the stress field was elastic. This means that the energy loss associated with crack extension occurs only at the mathematical point which represents the location of the leading edge of the crack. Actually we know that the energy devoted to fracturing is mainly dissipated into heat within a region of non-elastic strains adjacent to the leading edge of the crack. Presumably some gain in analysis accuracy would

* see page 6

result if we moved the point position of the leading edge into a central location within the region of non-elastic strains. This can be remembered for future consideration. For the present, it will be assumed that the lateral dimensions of the non-elastic or "plastic" zone are negligible.

Obviously the term $P\,d\Delta$ in equation (3) must be generalized if there are a number of loading force positions. Otherwise equation (3) defines $\mathcal{G}$ for a situation which is not "system isolated". Assume next that the stress strain relations applicable to the stress field are linear-elastic. This means that the load displacement, Δ, is directly proportional to the load.

$$\Delta = C\,P \qquad (d\Delta = C\,dP + P\,dC) \tag{4}$$

where C isthe compliance. Furthermore

$$U_T = \frac{1}{2} P\,\Delta \tag{5}$$

From equation (4)

$$P\,d\Delta = \Delta\,dP + P^2 dC \tag{6}$$

From equation (5)

$$d\,U_T = \frac{1}{2}\,(\Delta\,dP + P\,d\Delta) \tag{7}$$

Using equations (6) and (7) in (3), provides

$$\mathcal{G} = \frac{P^2}{2B}\,\frac{dC}{da} \tag{8}$$

C is an increasing function of the crack size, a. For a fixed crack size, C and $\frac{dC}{da}$ do not depend upon P and Δ.

Values of $\mathcal{G}$ can be determined for plate specimens, such as that pictured in Figure 1, using equation (8). Values of C are first measured as a function of the crack size, a, using small loads (to avoid non-linear strains; and a series of notch depths to represent a spaced sequence of a values. Methods of curve fitting and trend analysis can be used to plot accurate graphs of C and dC/da as functions of a. With this information at hand,

crack extension experiments can be done using similar specimens and the $\mathcal{G}$ values of interest can be calculated from observations of parameter pairs such as P,a; P,Δ; P,C; and Δ,C. The procedure described above is termed a compliance calibration.

The test specimen shown in Figure 2 is termed a double-cantilever- beam (DCB) specimen. Such specimens are useful in measurements of the tensile cracking strength of adhesive joints. The upper and lower halves of the specimen serve as the adherends. The separation is confined to the thin layer of adhesive between the adherends. In this figure the leading edge of the crack is shown as at a distance, a, from the loading line. The beam height of each adherend is h. As before, the specimen thickness across the leading edge of the crack is B. If each adherend is regarded as a beam which is "built-in" at the position of the crack tip, an equation from Timoshenko provides the following estimate of Δ;

$$\frac{\Delta}{2} = \frac{Pa^3}{3EI} + \frac{3}{2}\frac{Pa}{\mu hB} \qquad (9)$$

Since the second term on the right is usually small, we will assume

$$E = 2\mu(1 + \nu) = \frac{8}{3}\mu \qquad (10)$$

corresponding to $\nu = 1/3$.

Equation (9) can then be written in the form

$$\Delta = \frac{2P}{3EI}(a^3 + h^2a) \qquad (11)$$

Because the adhering beams are actually built-in only at their contacting surfaces, the observedload deflections will correspond to beam lengths larger than a by a moderate fraction of h which will be termed, a_o. Thus

$$C = \frac{2}{3EI}\left[(a+a_o)^3 + h^2(a+a_o)\right] \qquad (12)$$

$$\frac{dC}{da} = \frac{8}{EB}\left[\frac{3(a+a_o)^2}{h^3} + \frac{1}{h}\right] \qquad (13)$$

when a is much larger than h, equation (13) with the choice, $a_o = \frac{h}{3}$, often provides satisfactory accuracy. However, in actual use of DCB specimens, a compliance calibration is desirable in order to determine the best choice of a_o as well as the range of a-values for which an equation similar to equation (13) can be used.

Study of the dependency of the load displacements on a and h suggests that dC/da, for any given value of a, depends primarily on the beam height near the crack tip location. This fact suggested the development of contoured DCB specimens* in which the variation in beam height was adjusted so that dC/da remains fixed with changes of crack size. Contoured DCB specimens are of special value for experiments in which only load observations are feasible and for experiments in which a constant value of $\mathcal{G}$ by application of a fixed load is wanted.

For the purpose of investigations of crack extension in nearly isotropic solids, specimens of the DCB type are handicapped by the tendency of the crack to turn and break off one arm of the specimen. This difficulty can be overcome to a large extent by grooving the specimen faces along the line of desired crack extension. In this way the tensile stress near the crack tip parallel to the specimen length (due to bending) is reduced in comparison to the tensile stress normal to the desired locus of the plane of separation.

*S Mostovoy, P.B. Crosley, and E.J. Ripling "Use of Crack-Line-Loaded Specimens for Measuring Plane-Strain Fracture Toughness", Jnl. of Materials, Vol. 2, p. 661, (1967).

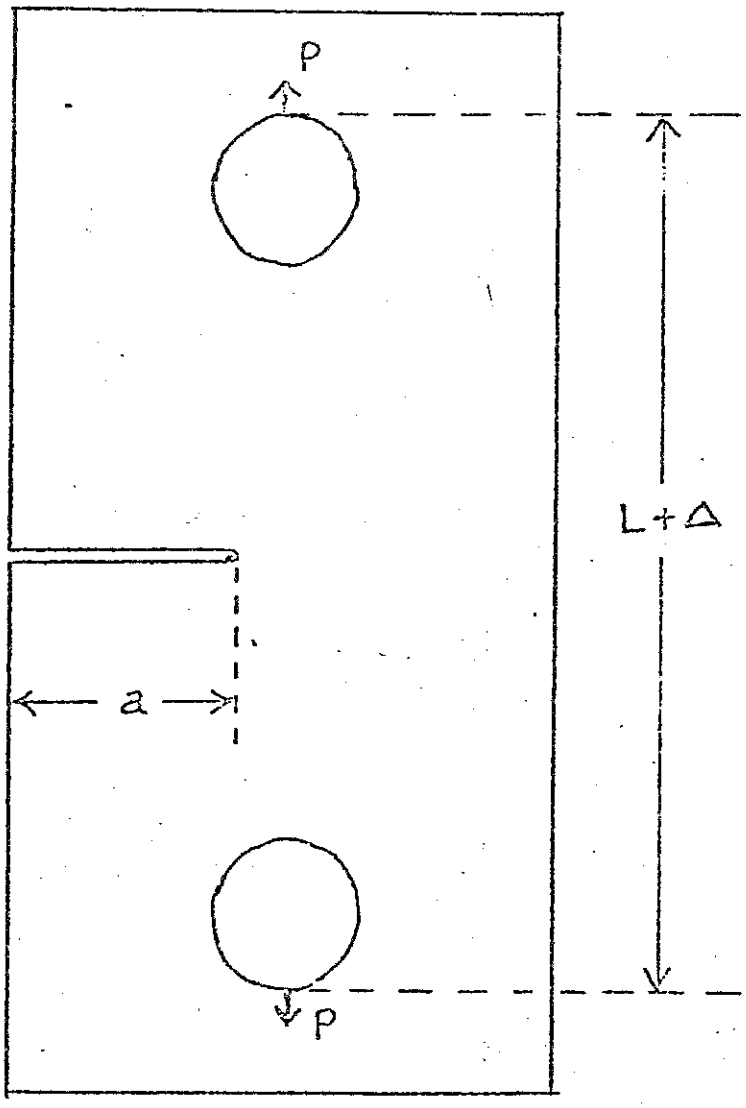

Figure 1. Edge Notched Tensile Specimen

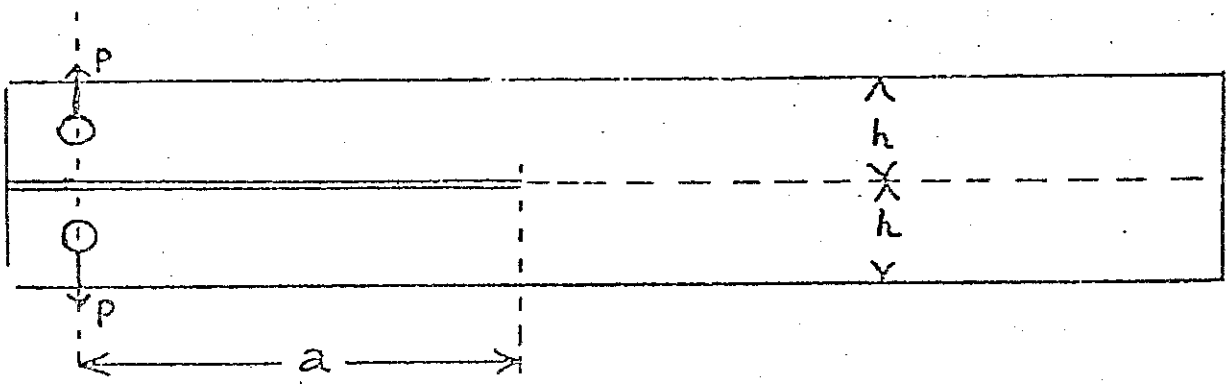

Figure 2. DCB Test Specimen

Consider a long uniform strip in tension as shown in Figure 3.

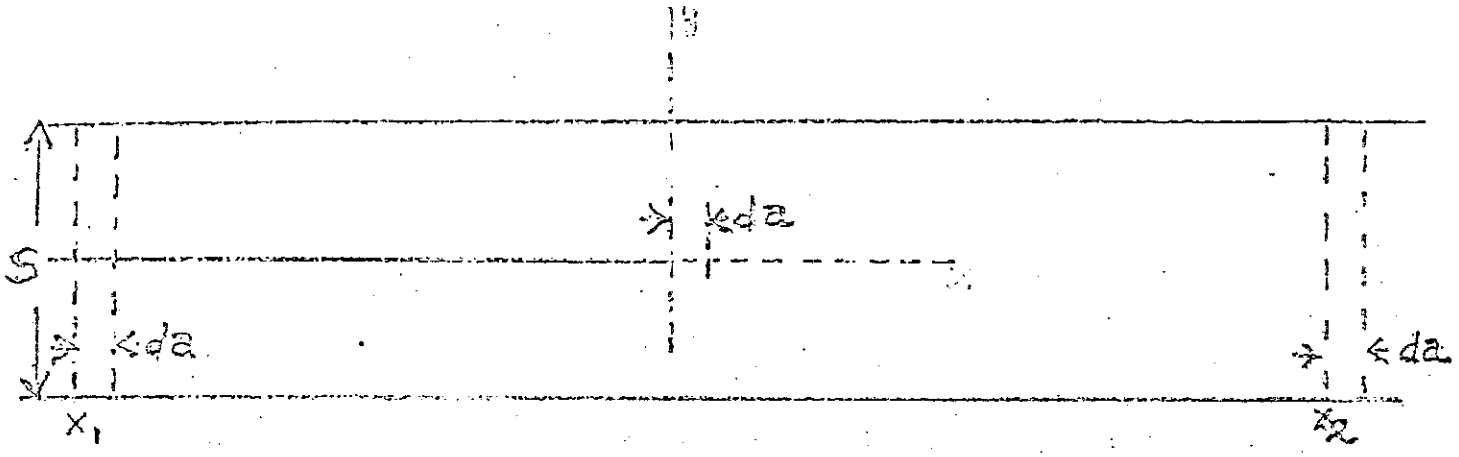

Figure 3 - Semi-infinite crack bisecting a strip of height S.

We imagine a crack was introduced out of view to the left and has advanced to the position shown. The original stress in the strip is assumed to be $\sigma_y = \sigma$ and $\sigma_x = 0$. The strip is assumed to be held at the upper and lower boundaries so that motion in the y-direction isprevented but also so that the condition $\sigma_x = 0$ is preserved. We can select arbitrary boundary lines, x_1 and x_2, such that to the right of x_2 the stresses do not differ significantly from the original stress condition, and so that to the left of x_1 the stresses do not differ significantly from zero. As the crack advances an additional increment, da, the boundary lines are imagined to move with the leading edge of the crack. In this way, one can see that the loss of stress field energy ~~(per unit thickness)~~ is simply the stress field energy between the two x_2 boundary line positions separated by da. Thus, on a unit thickness basis,

$$\mathcal{G}_{da} = \frac{\sigma^2}{2E} \quad (Sda) \tag{14}$$

and

$$\mathcal{G} = \frac{\sigma^2 S}{2E} \tag{15}$$

In the case of a long crack bisecting a strip (as illustrated above) as well as in crack problems solved using equation (8) (as illustrated by the DCB test specimen), the determination of $\mathcal{G}$ does not require a study of the stress intensification near the leading edge of the crack.

Actual cracking patterns for which equation (15) is useful can be observed when a plate of glass is broken so as to produce a spreading pattern of closely spaced cracks. At any given moment of time, the locus of the leading edges is a line drawn normal to the crack paths. In general, this line is curved and the stress, σ, is regarded as a notch root maximum stress with the locus line of the leading edges acting as the notch. Otherwise, the crack spacing can be taken as equivalent to S and equation (15) can be used to provide a static analysis estimate of the value of $\mathcal{G}$.

Two Dimensional Analysis of Cracks

A. The Airy Equation and the Airy Stress Function

Prior to direct treatment of crack problems, a brief review will be given of certain basic aspects of two-dimensional linear-elastic analysis. The solid under consideration can be regarded as a flat plate of uniform thickness and the material as being homogeneous, isotropic, and linear-elastic. The coordinates, x and y, are in the plane of the plate. A crack, when present will always be a straight through-the-thickness separation located on $y = 0$. Only static stress fields will be considered. Thus the inertia of the material plays no role in the equations for stress compatibility. The stress compatibility equations simply specify conditions on the stress gradients such that every small element of the material is in equilibrium. These equations are

$$\frac{\partial \sigma_x}{\partial x} + \frac{\partial \tau_{xy}}{\partial y} = 0$$
$$\frac{\partial \tau_{xy}}{\partial x} + \frac{\partial \sigma_y}{\partial y} = 0 \qquad (1)$$

One can easily see that equations (1) are always satisfied if

$$\sigma_x = \frac{\partial^2 F}{\partial y^2} \; ; \quad \sigma_y = \frac{\partial^2 F}{\partial x^2} \; ; \quad \tau_{xy} = - \frac{\partial^2 F}{\partial x \partial y} \qquad (2)$$

where F is a well behaved function of x and y.

The Hooke's law relationships which represent the linear-elastic nature of the material can be written (for plane-stress, $\sigma_z = 0$) in the form

$$E \epsilon_x = \sigma_x - \nu \sigma_y$$
$$E \epsilon_y = \sigma_y - \nu \sigma_x \qquad (3)$$
$$E \gamma_{xy} = 2(1+\nu) \tau_{xy}$$

where E is Young's Modulus and ν is Poisson's ratio.

$$\varepsilon_x = \frac{\partial u}{\partial x} \qquad \varepsilon_y = \frac{\partial v}{\partial y} \qquad \gamma_{xy} = \frac{\partial v}{\partial x} + \frac{\partial u}{\partial y}$$

It is desirable to make use of the fact that the three strains (ϵ_x, ϵ_y, γ_{xy}) are derived from only two displacements, the x-direction displacement, u, and the y-direction displacement v. The displacement compatibility relationship expressing this fact is given by

$$\frac{\partial^2 \epsilon_x}{\partial y^2} + \frac{\partial^2 \epsilon_y}{\partial x^2} = \frac{\partial^2}{\partial x \partial y} (\gamma_{xy}) \qquad (4)$$

If the stresses in equations (3) are replaced using equations (2), substitution of the strains from equations (3) in the equation (4) then gives the result

$$\frac{\partial^4 F}{\partial y^4} + \frac{2 \partial^4 F}{\partial x^2 \partial y^2} + \frac{\partial^4 F}{\partial x^4} = 0 \qquad (5)$$

This fourth order homogeneous partial differential equation for the function F is often written as

$$\nabla^2 (\nabla^2 F) = 0 \qquad (6)$$

where $\nabla^2 = \frac{\partial^2}{\partial y^2} + \frac{\partial^2}{\partial x^2}$ (7)

Equation (5) is the Airy equation and F is termed the Airy stress function.

Obviously any solution, φ, of the Laplace (harmonic) equation

$$\nabla^2 \varphi = 0 \qquad (8)$$

would be a solution of equations (5) and (6). However, these equations are of higher order (bi-harmonic) and one can show that the general solution can be written in the form

$$F = \varphi_1 + x\varphi_2 + y\varphi_3 + (x^2+y^2)\varphi_4 \qquad (9)$$

where the functions φ_i (i = 1, 2, 3, 4) are all solutions of equation (8). Such functions are often termed "harmonic" or "potential" functions.

It is not difficult to find illustrative harmonic functions. In fact either the real or the complex part of any function of the complex variable, $z = x + iy$,

satisfies equation (8). As an example consider the function $f(z) = \log z$. Since

$$z = re^{i\theta}, \quad \log z = \log r + i\theta \tag{10}$$

where $r^2 = x^2 + y^2$ and $\tan \theta = y/x$

Thus the real and imaginary parts of $\log z$ are given by

$$\mathrm{Re}(\log z) = \log r = 1/2 \log (x^2+y^2) \tag{11}$$

$$\mathrm{Im}(\log z) = \theta = \arctan (y/x) \tag{12}$$

Trial of the right sides of equations (11) and (12) in the Laplace equation readily shows that they are both harmonic functions.

After some practice in choosing functions which solve certain types of elastic stress field problems, an experienced analyst can "guess" appropriate harmonic functions, adjust coefficients to satisfy boundary conditions and produce stress field solutions by what is termed the "semi-inverse" method. The quickness of this procedure is attractive and it will be seen that stress field solutions for a large number of two-dimensional crack problems can be obtained by a relatively simple "semi-inverse" method.

B. The Westergaard Method

A technical paper by Westergaard (Trans. ASME, 1939, A, Vol. 61, p 49) presented an adaptation of equation (9) which is convenient for solving problems in which the crack is on $y = 0$, the plate size is infinite relative to the crack size, and the loading symmetry is such that $\tau_{xy} = 0$ on $y = 0$. Westergaard considered a restricted form of equation (9)

$$F = \varphi_1 + y\varphi_2 \tag{13}$$

and selected the harmonic functions φ_1 and φ_2 so that τ_{xy} would be zero when $y = 0$.

In order to understand and use the Westergaard method, it is desirable to understand how to obtain the x and y derivatives of Re(f) and Im(f) in a simple and rather general manner. Consider the following equations in which f is a function of $z = x + iy$.

Assuming $f(z) = \mathrm{Re}\, f + i\, \mathrm{Im}\, f$

$$\frac{\partial f}{\partial x} = \frac{\partial}{\partial x} \mathrm{Re}\, f + i \frac{\partial}{\partial x} \mathrm{Im}\, f = f' \tag{14}$$

$$f' = \mathrm{Re}\, f' + i\, \mathrm{Im}\, f' \tag{15}$$

$$\frac{\partial f}{\partial y} = \frac{\partial}{\partial y} \mathrm{Re}\, f + i \frac{\partial}{\partial y} \mathrm{Im}\, f = i f' \tag{16}$$

$$i f' = i\, \mathrm{Re}\, f' - \mathrm{Im}\, f' \tag{17}$$

Matching the real and imaginary parts of equations (14) and (15)

$$\frac{\partial}{\partial x} \mathrm{Re}\, f = \mathrm{Re}\, f' \; ; \; \frac{\partial}{\partial x} \mathrm{Im}\, f = \mathrm{Im}\, f' \tag{18}$$

Matching the real and imaginary parts of equations (16) and (17)

$$\frac{\partial}{\partial y} \mathrm{Re}\, f = -\mathrm{Im}\, f' \; ; \; \frac{\partial}{\partial y} \mathrm{Im}\, f = \mathrm{Re}\, f' \tag{19}$$

Equations (18) and (19), termed the Cauchy-Riemann relations, permit the writing out of x and y derivatives of $f(z)$ in a formal way prior to specific selection of $f(z)$.

Consider next the results of choosing

$$\phi_1 = \mathrm{Re}\, \bar{\bar{Z}} \quad \text{and} \quad \phi_2 = \mathrm{Im}\, \bar{Z} \tag{20}$$

Presumably in order to avoid use of high order derivative notations, Westergaard preferred to use the following terminology in which Z', Z, $\bar{Z}$, and $\bar{\bar{Z}}$ are all functions of the complex variable z,

$$Z' = \frac{d}{dz} Z \; , \; Z = \frac{d}{dz} \bar{Z} \; , \; \bar{Z} = \frac{d}{dz} \bar{\bar{Z}} \tag{21}$$

Starting with equation (13) in the form

$$F = \mathrm{Re}\, \bar{\bar{Z}} + y\, \mathrm{Im}\, \bar{Z} \tag{22}$$

and using equations (2), (18), and (19), one finds that

$$\sigma_y = \mathrm{Re}\, Z + y\, \mathrm{Im}\, Z' \tag{23}$$

$$\sigma_x = \mathrm{Re}\, Z - y\, \mathrm{Im}\, Z' \tag{24}$$

$$\tau_{xy} = -y\, \mathrm{Re}\, Z' \tag{25}$$

One can easily see that if ReZ' is bounded on $y = 0$, then τ_{xy} is zero on $y = 0$. Thus, for crack problems such that $\tau_{xy} = 0$ on $y = 0$, equation (22) reduces the semi-inverse method to the choice of a single stress function, $Z(z)$. There is, of course, some question as to whether this degree of simplification of equation (9) is overly restrictive in terms of the crack problems which can be solved. With regard to this aspect two comments are appropriate. (1) The restriction to problems such to $\tau_{xy} = 0$ on $y = 0$ is easily removed by a simple modification of equation (22) such that $\tau_{xy} = 0$ on $y = 0$ is replaced by $\sigma_y = 0$ on $y = 0$. This permits treatment of a large range of crack problems with in-plane loading. (2) From experience, crack stress field problems divide into two classes. Those which require numerical approximation methods (use of a computor program), and those which have relatively simple closed form solutions. With rare exceptions all of the solutions of the second kind are obtainable using the Westergaard method. Even when a numerical approximation method is necessary, the Westergaard method is usually helpful in establishing the computational program.

C. Illustrative Two-Dimensional Crack Problems

In 1913 Inglis published a solution for the stresses near a two-dimensional elliptical opening in an infinite plate subjected to a uniform bi-axial stress field remote from the opening. In order to obtain the stress field for a small crack in a field of tension normal to the crack, Griffith (1920) increased the eccentricity of the elliptical opening so that the minor axis approached zero.

Using the Westergaard approach the answers sought by Griffith are obtained by the choice

$$Z = \frac{\sigma}{\sqrt{1-(a/z)^2}} \qquad (26)$$

Here the crack extends from x = -a to x = a on y = 0. In order to see that this choice is satisfactory with regard to boundary conditions, re-write equation (26) in its first quadrant form

$$Z = \frac{\sigma z}{\sqrt{z^2 - a^2}} \qquad (27)$$

and substitute vectors for z, (z-a), and (z+a) as follows

$$z = r e^{i\theta} \quad , \quad z - a = r_1 e^{i\theta_1} \quad , \quad z + a = r_2 e^{i\theta_2} \qquad (28)$$

These vectors are shown in figure 1

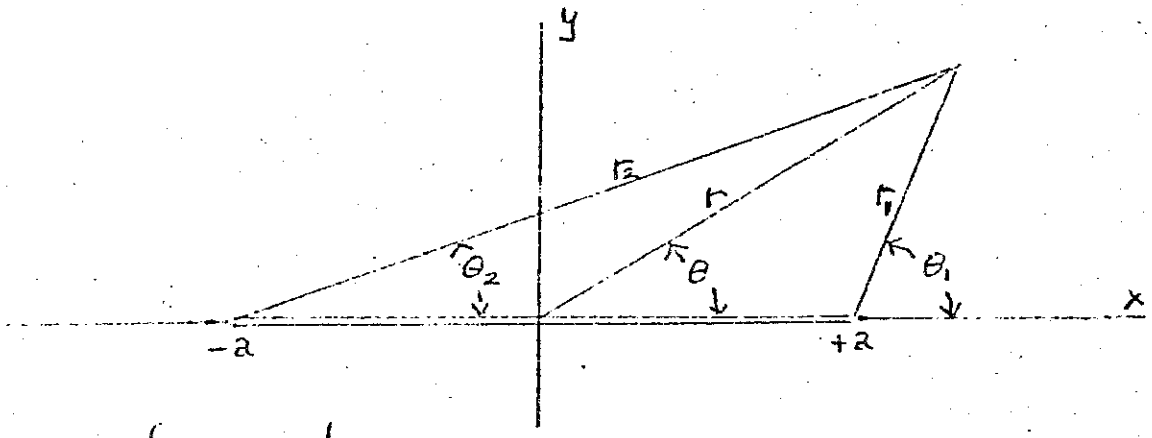

figure 1

Differentiating equation (26) or (27), gives

$$Z' = \frac{-\sigma a^2}{(z^2 - a^2)^{3/2}} \qquad (29)$$

Using the vector notation

$$Z = \frac{\sigma r}{\sqrt{r_1 r_2}} e^{i\left\{\theta - \frac{\theta_1 + \theta_2}{2}\right\}}$$

$$= \frac{\sigma r}{\sqrt{r_1 r_2}} \left[\cos\left\{\theta - \frac{\theta_1 + \theta_2}{2}\right\} + i \sin\left\{\theta - \frac{\theta_1 + \theta_2}{2}\right\}\right] \qquad (30)$$

$$Z' = \frac{-\sigma a^2}{(r_1 r_2)^{3/2}} e^{-i\frac{3}{2}(\theta_1+\theta_2)}$$

$$= \frac{-\sigma a^2}{(r_1 r_2)^{3/2}} \left[\cos\frac{3}{2}(\theta_1+\theta_2) - i\sin\frac{3}{2}(\theta_1+\theta_2)\right] \qquad (31)$$

If we agree to restrict the angles θ, θ_1, and θ_2 to the range $-\pi$ to π, then equations (30) and (31) retain the symmetry implied by equation (26). Referring to equations(23), (24), and (25) one can see that ReZ = σ in the limit as r approaches infinity for all values of θ. In addition the terms yReZ' and yImZ' approach zero as r approaches infinity for all values of θ. Thus the applied load at infinity is $\sigma_y = \sigma_x = \sigma$. If we wish to modify this stress field toward $\sigma_x = 0$ at large r, this can be done by adding a uniform x-direction compressive stress.

Consider next the boundary conditions on y = 0 with x between -a and +a. Along this region the crack surfaces must be free relative to the stresses σ_y and τ_{xy}. The crack line region can be specified by taking $\theta = 0$ or π, $\theta_1 = \pi$ and $\theta_2 = 0$. τ_{xy} is zero because yReZ' is zero. σ_y is given by ReZ and is zero because

$$\cos\left(\theta - \frac{\theta_1+\theta_2}{2}\right) = \cos\frac{\pi}{2} = 0 \quad (\text{for } \theta = \pi) \qquad (32)$$

$$= \cos\left(-\frac{\pi}{2}\right) = 0 \quad (\text{for } \theta = 0)$$

In most cases, a check of the boundary conditions with regard to stress as indicated above, provides an adequate guarantee that we have obtained a complete and unique solution of the particular crack problem under examination. However, as a matter of caution with regard to having the proper solution, it is usually desirable to examine the behavior of the displacements as well as the behavior of the stresses. Referring to equations (3) and substituting from equations (23) and (24), one finds

$$E\,\varepsilon_x = E\,\frac{\partial u}{\partial x} = (1-\nu)\,\mathrm{Re}\,Z - (1+\nu)\,y\,\mathrm{Im}\,Z' \qquad (33)$$

$$E\,\varepsilon_y = E\,\frac{\partial v}{\partial y} = (1-\nu)\,\mathrm{Re}\,Z + (1+\nu)\,y\,\mathrm{Im}\,Z' \qquad (34)$$

The integrals of these equations are given by

$$E\,u = (1-\nu)\,\mathrm{Re}\,\bar{Z} - (1+\nu)\,y\,\mathrm{Im}\,Z \qquad (35)$$

$$E\,v = 2\,\mathrm{Im}\,\bar{\bar{Z}} - (1+\nu)\,y\,\mathrm{Re}\,Z \qquad (36)$$

From examination of equation (27), the integral of $Z(z)$ which is termed $\bar{Z}$ is given by

$$\bar{Z} = \sigma\sqrt{z^2-a^2} \qquad (37)$$

Remote from the crack the displacements increase toward infinity in linear fashion as would be expected. On $y = 0$

$$\bar{Z} = \sigma\sqrt{x^2-a^2} \qquad (38)$$

clearly $\mathrm{Im}\bar{Z}$ and v are zero on $y = 0$ unless $|x| \leq a$, again the expected behavior. Along the line segment occupied by the crack the value of v is the half-opening, η is given by the equation

$$E\,\eta = 2\sigma\sqrt{a^2-x^2} \qquad (39)$$

It can be observed that a trace of the crack opening, with η enlarged to finite size, would have the shape of an ellipse. The major semi-axis of the ellipse is

& and the minor semi-axis is η_o where

$$\eta_o = \frac{2\sigma a}{E}$$

It is of some interest to note the size of the small root radius, ρ, of the crack opening at the end regions of the crack.

$$\rho = \eta_o^2/a = 4\left(\frac{\sigma}{E}\right)^2 a \qquad (41)$$

In the establishment of linear-elastic relationships from fundamental concepts it is necessary to regard strains as infinitesimal in comparison to unity. This means that σ/E can be regarded as infinitesimal, and that ρ is a second order infinitesimal in comparison to the half-length, a, of the crack.

Leading Edge Stress Equations

In order to examine the stresses very close to the right leading edge of the crack discussed above (equ. 27), put $\zeta = a + \zeta_1$ and consider a small region within which $|\zeta_1|$ is as small as we please in comparison to the half-length, a, of the crack.

Thus $\zeta = a + \zeta_1 \cong a$ (42)

$\zeta - a = \zeta_1$ (43)

$\zeta + a = 2a + \zeta_1 \cong 2a$ (44)

Substituting these into equation (27),

$$Z \cong \frac{\sigma a}{\sqrt{2a\zeta_1}} = \frac{\sigma\sqrt{\pi a}}{\sqrt{2\pi\zeta_1}} \qquad (45)$$

The reason for inserting $\sqrt{\pi}$ above and below the division line of equation (45) will be explained at a later point. Examination of equation (45) indicates that the stress field near the crack tip can be derived directly from the stress function

$$Z = \frac{K}{\sqrt{2\pi\zeta}} \qquad (46)$$

where $K = \sigma\sqrt{\pi a}$. Dropping the subscript from ζ_1 is simply equivalent to shifting the origin of the x, y coordinates to the crack tip.

Differentiating equation (46)

$$Z' = \frac{-K}{2\sqrt{2\pi}\,(\zeta)^{3/2}} \qquad (47)$$

$$= \frac{-K}{2r\sqrt{2\pi r}}\, e^{-\frac{3}{2}\theta}$$

$$= -\frac{K}{2r\sqrt{2\pi r}}\left(\cos\frac{3\theta}{2} - i\sin\frac{3\theta}{2}\right) \qquad (48)$$

From equation (48) and $y = r \sin\theta$,

$$y \operatorname{Im} Z' = \frac{K}{\sqrt{2\pi r}} \frac{\sin\theta}{2} \sin\frac{3\theta}{2}$$

$$= \frac{K}{\sqrt{2\pi r}} \sin\frac{\theta}{2} \cos\frac{\theta}{2} \sin\frac{3\theta}{2} \qquad (49)$$

From equation (46)

$$\operatorname{Re} Z = \frac{K}{\sqrt{2\pi r}} \operatorname{Re}\left(e^{-i\frac{\theta}{2}}\right)$$

$$= \frac{K}{\sqrt{2\pi r}} \cos\frac{\theta}{2} \qquad (50)$$

Using equations (23) and (24),

$$\sigma_y = \frac{K}{\sqrt{2\pi r}} \cos\frac{\theta}{2} \left\{1 + \sin\frac{\theta}{2} \sin\frac{3\theta}{2}\right\} \qquad (51)$$

$$\sigma_x = \frac{K}{\sqrt{2\pi r}} \cos\frac{\theta}{2} \left\{1 - \sin\frac{\theta}{2} \sin\frac{3\theta}{2}\right\} \qquad (52)$$

Referring again to equation (48),

$$\tau_{xy} = -y \operatorname{Re} Z' = \frac{K}{\sqrt{2\pi r}} \sin\frac{\theta}{2} \cos\frac{\theta}{2} \cos\frac{3\theta}{2} \qquad (53)$$

In the limit of a close enough approach to the crack tip, equations (51), (52), and (53) furnish a stress pattern which is characteristic for the leading edge of any opening mode or tensile crack. The term, opening mode, means that the stresses τ_{xy} and τ_{yz} are zero on $\theta = 0$ directly ahead of the crack tip. In order to assist examination of this pattern, it is helpful to have the equations

for the principal stresses, σ_1, and σ_2. These can be obtained using the relations,

$$\sigma_1 = \frac{\sigma_y + \sigma_x}{2} + \sqrt{\left(\frac{\sigma_y - \sigma_x}{2}\right)^2 + \tau_{xy}^2} \tag{54}$$

$$\sigma_2 = \frac{\sigma_y + \sigma_x}{2} - \sqrt{\left(\frac{\sigma_y - \sigma_x}{2}\right)^2 + \tau_{xy}^2} \tag{55}$$

Using equations (51) and (52),

$$\sigma_1 = \frac{K}{\sqrt{2\pi r}} \cos\frac{\theta}{2}\left(1 + \sin\frac{\theta}{2}\right) \tag{56}$$

$$\sigma_2 = \frac{K}{\sqrt{2\pi r}} \cos\frac{\theta}{2}\left(1 - \sin\frac{\theta}{2}\right) \tag{57}$$

From the above pair ofequations, the maximum shear stress, τ_M, is given by

$$\tau_M = \frac{\sigma_1 - \sigma_2}{2} = \frac{K}{\sqrt{2\pi r}} \frac{\sin\theta}{2} \tag{58}$$

If a plate of photo-elastic sensitive material containing a crack is subjected to tension normal to the crack, a simple arrangement of lighting and light polarizing elements permits examination of lines in the plate along which τ_M has a constant value. These are termed isochromatic lines. Using equation (58), one can readily find that, close to the crack tip, these lines resemble closed ovaloids as shown in Figure 2.

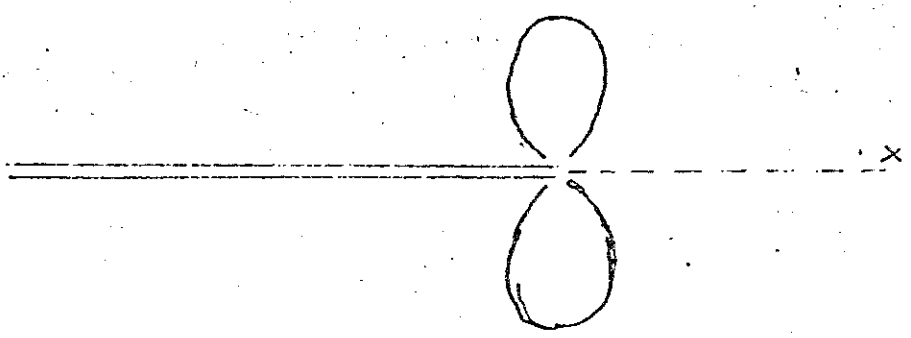

Figure 2

A study of equation (56) discloses that the largest tensile stress at any fixed distance, r, from the crack tip occurs when $\theta = \pm \pi/3$ ($\theta = \pm 60^{o}$). The commonly observed mechanism of progressive crack extension consists in the opening and subsequent joining of advance separations. In the structural metals, the advance separations lie close to the crack tip enclosed in a region where the stress-strain relations are non-linear. However, if we ignore this complexity and consider only the expected influence of the linear-elastic stress pattern on texture and trajectory of a crack, several observations of interest can be noted. The tendency of the stress pattern to encourage development of advance origins which lie above or below the x-axis is in appropriate correspondence to the rough texture commonly observed in flat-tensile fracturing of structural metals. Secondly, if the joining process moves the crack tip region upward, the influence of this event on the stress pattern favors a downward movement of the next segment of fracturing. Thus the average trajectory of the crack is expected to remain normal to the greatest tension.

It is of special interest that all three stresses ($\sigma_x, \sigma_y, \tau_{xy}$) close to the crack tip are proportional to the value of K. In the case of the central crack corresponding to the function Z(z) given by equation (26), K was equal to $\sigma\sqrt{\pi a}$. For other opening mode crack problems it will be found that equation (46) continues to provide the stress pattern close to the crack tip. The relationship one would use to compute the stress intensity factor, K, depends, of course, on the nature of the crack problem under consideration.

The stress fields corresponding to the two functions, Z(z), given by equations (26) and (46) have now been discussed. Consider next a central crack opened by forces applied at the crack line as shown in Figure (3).

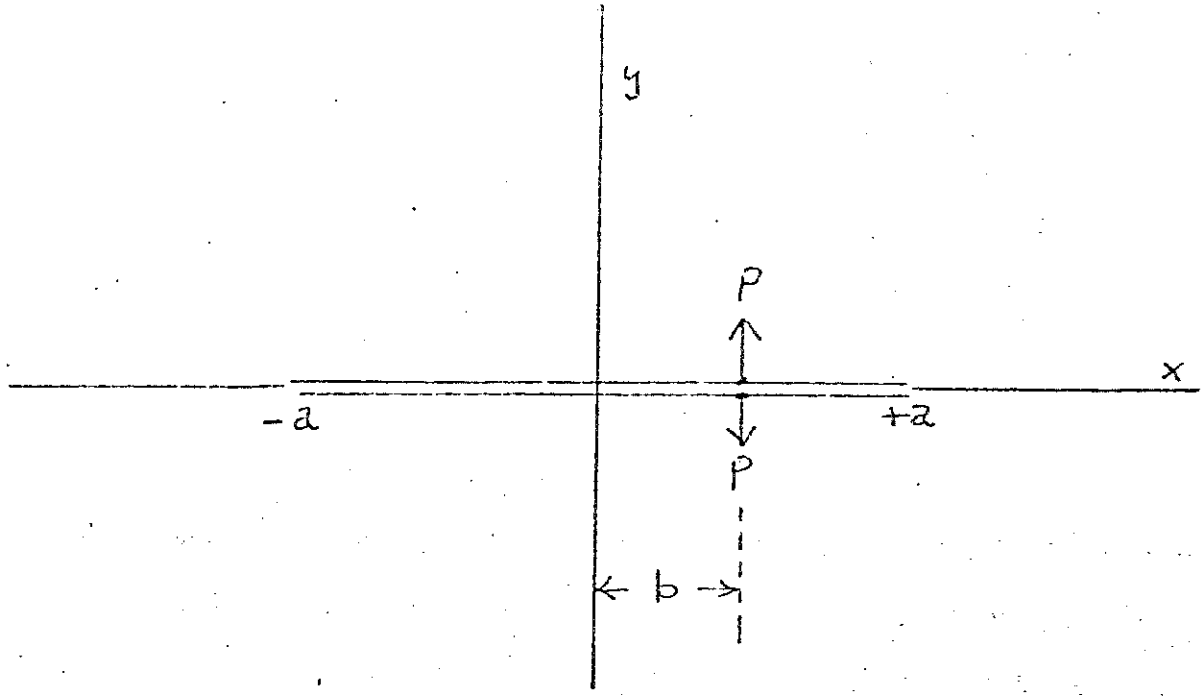

Figure 3

In order to "guess" the function $Z(z)$ which provides the stress field it is helpful to examine the Z function suggested by Westergaard (1939) as representing a line force acting at the origin of the x, y coordinates ... upward against the lower boundary of a semi-infinite plate.

$$Z = \frac{P}{i\pi z} = -\frac{P}{\pi r}(\sin\theta + i\cos\theta) \qquad (59)$$

$$\bar{Z} = \frac{P}{i\pi}\log z = \frac{P}{i\pi}(\log r + i\theta) \qquad (60)$$

From equation (59), ReZ = 0 both on $\theta = 0$ and on $\theta = \pi$. Thus the x-axis is a free boundary. In order to verify the presence of the force, P, consider the downward force exerted by the stress field across a line around the force locat... as shown in Figure 4.

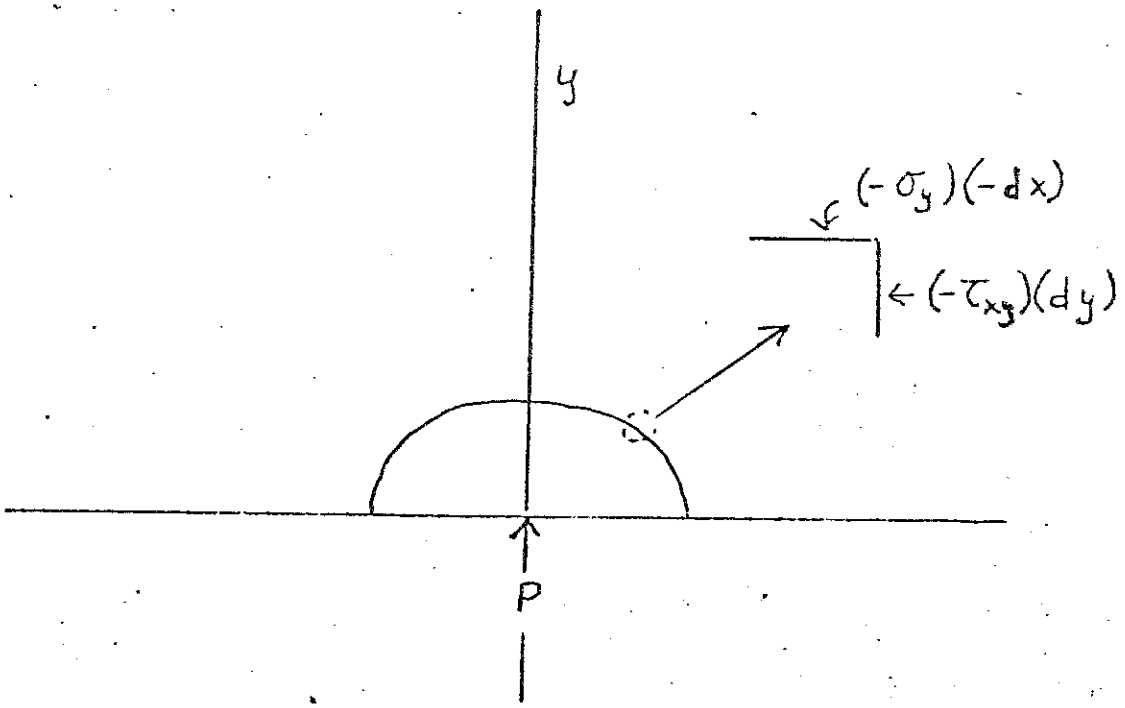

Figure 4

The direction of integration along the arbitrary line is counter-clockwise. The line can be regarded as composed of segments dy and dx as shown in the figure. The stress field must exert a downward force given by

$$P = \oint_{\theta=0}^{\theta=\pi} (\sigma_y\, dx - \tau_{xy}\, dy) \tag{61}$$

$$= \oint \left[\frac{\partial}{\partial x}\left(\frac{\partial F}{\partial x}\right) dx + \frac{\partial}{\partial y}\left(\frac{\partial F}{\partial x}\right) dy \right] \tag{62}$$

$$= \oint d\left(\frac{\partial F}{\partial x}\right) \tag{63}$$

From equation (63)

$$P = \left[Re\,\bar{Z} + y\, Im\, Z \right]_{\theta=0}^{\theta=\pi} \tag{64}$$

However, from equation (60), $Re\bar{Z}$ is $P\theta/\pi$. Thus the form of Z given by equation (59) is correct.

With regard to the forces on the crack line shown in Figure 3, the force location is easily shifted to x = b by substitution of $(\zeta - b)$ for ζ in equation (59). With this in mind and recognizing that inverse square-root singularities should be present at the crack tip locations, we can try the Z value given by

$$Z = \frac{P}{\pi(\zeta - b)} \frac{\sqrt{a^2 - b^2}}{\sqrt{\zeta^2 - a^2}} \tag{65}$$

In the close vicinity of y = 0, x = b, ζ is nearly equal to b. Thus

$$Z \cong \frac{P}{i\pi(\zeta - b)} \tag{66}$$

Furthermore a careful examination of ReZ above and below y = 0, x = b using the vector notation form of equation (65) shows compressive stresses, corresponding to application of a downward force P against the lower surface of the crack as well as to upward action of a force P against the upper surface of the crack. From the nature of equation (65) there are no loads at infinity. Thus the stress type boundary conditions of the problem are satisfied. In order to examine the stress pattern near the crack tip at x = a, substitute into equation (65) the relations

$$\zeta - b \cong a - b$$

$$\zeta + a \cong 2a$$

$$\zeta - a = \zeta_1$$

The result can be written in the following way:

$$Z \cong \frac{P}{\sqrt{\pi a}} \sqrt{\frac{a+b}{a-b}} \frac{1}{\sqrt{2\pi\zeta_1}} \tag{67}$$

Equation (67) has the same form as equation (45). Thus the crack tip stress pattern can be derived as before starting with equation (46) and using the K value given by

$$K = \frac{P}{\sqrt{\pi a}} \sqrt{\frac{a+b}{a-b}} \tag{68}$$

Note that P has the dimensions of force per unit of plate thickness. Thus, as before, the dimensions of the stress intensity factor K are those of stress times the square-root of a length.

Suppose next that the loads are applied remotely from the central crack, in a symmetrical pattern so that $\tau_{xy} = 0$ on $y = 0$ but also so that σ_y on $y = 0$ would not be uniform even in the absence of the crack. Imagine first that the stress field problem is solved considering no crack present so that σ_y on $y = 0$ is a known function of x. We can now take the view that the central crack is present but is held closed by normal tensions, σ_y dx, on the crack surfaces given by the known function, $\sigma_y = \sigma_y(x)$. In order to establish free surface conditions along the crack line we can add to the existing stress field the stress field derived from

$$Z(\zeta) = \frac{1}{\pi\sqrt{\zeta^2 - a^2}} \int_{-a}^{+a} \frac{\sqrt{a^2 - x^2}}{\zeta - x} \sigma_y(x)\, dx \tag{69}$$

In equation (69), equation (65) is employed (with $P = \sigma_y$ dx) in order to cancel the normal tensions, σ_y dx, along the crack line by application of equal magnitude pressures. Since the streases introduced by the stress field corresponding to equation (69) are zero remote from the crack, the addition of this stress field requires no alteration of the initial loads which were assumed to be

remotely applied. The additivity of linear-elastic stress fields implies additivity of the K values. No contribution to K is made by the initial stress field calculated ignoring the crack because this stress field has no singularities at the crack tips. The total K value therefore must be given by the integral of equation (68) with $P = \sigma_y(b)\, db$.

$$K = \frac{1}{\sqrt{\pi a}} \int_{-a}^{a} \sqrt{\frac{a+b}{a-b}}\, \sigma_y(b)\, db \qquad (70)$$

Equation (70) gives the K value for the stress pattern near y = 0, x = a. For the region near the crack tip at y = 0, x = -a, the fraction inside the radical sign in equation (70) must be inverted.

Since the stress pattern derived from $Z = K/\sqrt{2\pi z}$ is characteristic for the crack tip region of any opening mode crack, and if we assume the non-linear zone containing the fracturing process is relatively small, it is clear that similar crack extension behaviors should be observed when the K values are similar, assuming no change in the material, loading speed, temperature, or plate thickness. Thus the value of K serves as a characterization of the tendency of the loading forces to cause forward motion of the fracturing process. It can be noted that this characterization may be incomplete since uniform stress fields parallel to x and to z can be added without changing the value of K. However, the available experimental evidence has not so far disclosed a significant effect of such added stress fields upon the control of the fracturing process by the K value. Using equation (51), the stress intensity factor K can be defined as follows:

$$K = \text{Limit}\ \left(\sigma_y \sqrt{2\pi r}\right) \qquad (71)$$
$$\text{as } r \to 0 \text{ on } \theta = 0$$

where σ_y is regarded as a function of r and r designates the distance from the crack tip of a point directly ahead on the line of expected crack extension.

The Proportionality of K^2 to $\mathcal{G}$

The preceding discussion assumed that the material is elastic. Within an elastic material a stress field change due to crack extension may cause transfer of stress field energy from one element to adjacent elements. Loss or disappearance of stress field energy cannot occur within the material itself. On the other hand, because of the stress singularity at the crack tip, the mathematical point-locus of the crack tip acts as an energy "sink". From the nature of the assumed analysis model, the energy disappearance associated with crack extension occurs exactly at the tip (or leading edge) of the crack. From these facts, a study of the rate of energy loss with crack extension in terms of stresses and displacements can be done using the stress and displacement equations which apply only in the close vicinity of the crack tip. Correspondingly the stresses in this region can be derived from the Westergaard stress function of equation (46);

$$Z = K/\sqrt{2\pi z} \tag{46}$$

Integrating equation (46)

$$\overline{Z} = \frac{K}{\pi}\sqrt{2\pi z} \tag{72}$$

The rate of disappearance of stress field energy per unit of new separational area, $\mathcal{G}$, can be calculated using the stress, σ_y given by equation (46) and the crack opening displacements, η, derived from equation (72). The plan of this calculation is to computethe work done in closing a very small segment, α, of the crack opening adjacent to the crack tip. The upper half of the crack tip region before and after this closure action is shown in Figure 5.

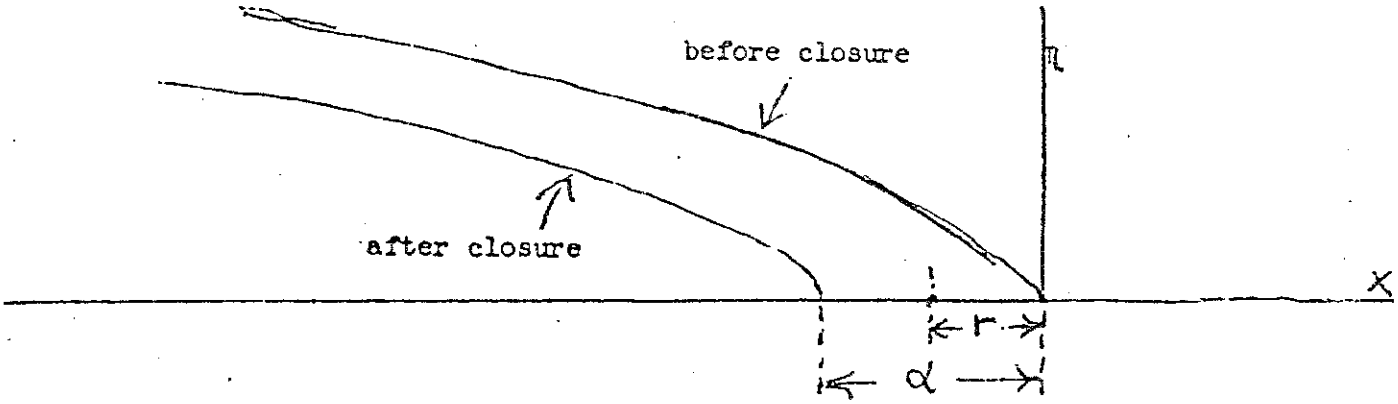

Figure 5

From Equations (36) and (72) the value of η on $y = 0$. $\theta = \pi$, before closure is given by

$$E\eta = 2\ \mathrm{Im}\bar{Z} = \frac{2K}{\pi}\sqrt{2\pi r} \tag{73}$$

After closure, the tensile force per unit thickness, $\sigma_y dr$, acting at the position, r, is given by

$$\sigma_y dr = \frac{K\,dr}{\sqrt{2\pi(\alpha-r)}} \tag{74}$$

Equation (74) assumes the closure segment is too small to alter the value of K. In addition the stress relationship must be based upon the distance from the crack tip after closure. This distance is $(\alpha-r)$. We assume each strip of width, dr, is closed simultaneously by the application of tensile forces proportional to those given by equation (74). Then from physical reasoning each closure force changes from zero to $\sigma_y dr$ in direct proportion to the closure displacement. Thus the closure work within each strip is $\frac{1}{2}\eta\sigma_y dr$. However, closure from below as well as above must be counted. Thus the total closure work per unit thickness, which is $\alpha\,\mathcal{G}$, is given by

$$\alpha \mathcal{G} = \int_0^\alpha \eta \, \sigma_y \, dr \qquad (75)$$

$$= \frac{2K^2}{\pi E} \int_0^\alpha dr \sqrt{\frac{r}{\alpha - r}}$$

Putting $r = \alpha \sin^2 u$ assists evaluation of the integral. One finds

$$\alpha \mathcal{G} = \alpha K^2/E \qquad (76)$$

The conclusion is that $K^2 = E \mathcal{G}$. On page 10 of these notes a factor, $\sqrt{\pi}$, was inserted into equations (45) and (46) with the promise of subsequent explanation. Neglecting certain historical aspects which are of minor interest here, the primary reason was the simplicity of the proportionality factor between K^2 and $\mathcal{G}$.

The validity of the above derivation, based upon the work done during closure of a small segment at the crack tip, might be questioned because the region of closure appears to be just the region of large strains and large rotations within which the methods of linear-elastic analysis should be excluded as not applicable. In answer to questions of this nature, it was noted previously that a formal calculation of the crack tip root radius, ρ, shows this length factor to be a second order infinitesimal relative to the crack size. Thus the region of large strains and large rotations, which is comparable in size to ρ, can be excluded as negligible in comparison to the size of α.

As an example of the equation, $K^2 = E \mathcal{G}$, it was shown that $K = \sigma \sqrt{\pi a}$ for a central crack of length, 2a, with a normal tensile stress, σ, applied remote from the crack. This is the crack problem which was employed by Griffith in his 1920 theory of fracture strength and the value of $\mathcal{G}$ is known to be given by

$$\mathcal{G} = \frac{\sigma^2 \pi a}{E} \qquad (77)$$

Thus it is clear that $K^2 = E\,\mathcal{G}$ for this particular problem. Because of the similarity of the stress-strain pattern near the crack tip for any opening mode crack, one would expect the proportionality factor between K^2 and $\mathcal{G}$ would be the same for any opening mode crack. The previously discussed calculation of crack closure work provided a proof of this expectation in analysis form.

It should be noted that equations (36) and (73) assumed plane-stress. If we had assumed plane-strain, the value of E in equation (73) would have been replaced by $E/(1-\nu^2)$. Thus the proportionality of K^2 to $\mathcal{G}$ for opening mode cracks is given by

$$K^2 = E_1\,\mathcal{G} \tag{78}$$

where $E_1 = E$ (plane-stress)

and $E_1 = E/(1-\nu^2)$ (plane-strain).

Although Mode II and Mode III crack problems are of secondary interest here, as a matter of completeness it may be noted that $K^2_{II} = E_1\,\mathcal{G}_{II}$ and $K^2_{III} = 2\mu\,\mathcal{G}_{III}$.

Crack Stress Fields Obtained by Addition and Integration

In this discussion reference will be made to portions of a set of lecture notes entitled "Supplementary Crack Stress Field Analysis Notes". For convenience these supplementary notes will be termed reference A. Consider first the Westergaard stress functions, Z_5 and Z_6 of reference A. From the figures accompanying these functions one would expect that Z_6 could be obtained from Z_5 by the addition

$$Z_5(z, a, b) + Z_5(z, a, -b) = Z_6(z, a, b) \tag{72}$$

Similarly one would expect to find that

$$\bar{Z}_5(\bar{z}, a, b) + \bar{Z}_5(\bar{z}, a, -b) = \bar{Z}_6(\bar{z}, a, b) \tag{73}$$

Verification of equation (72) is relatively simple using the equation

$$\frac{1}{z-b} + \frac{1}{z+b} = \frac{2z}{z^2-b^2} \tag{74}$$

Verification of equation (73) only requires recollection of the fact that

$$\arctan(f) = -\arctan(-f) \tag{75}$$

Consider next the problem of a central crack opened by a uniform pressure, σ, acting against the upper and lower surfaces of the crack. From the nature of this problem, a plausible "guess" of the appropriate Westergaard stress function is

$$Z = \frac{\sigma}{\sqrt{1-(a/z)^2}} - \sigma \tag{76}$$

From integration of equation (76),

$$\bar{Z} = \sigma\sqrt{z^2-a^2} - \sigma z \tag{77}$$

Examination of the stresses and displacements derived from these functions shows that they do, in fact, provide correct stresses and displacements for the above stated problem. Furthermore, since the constant term, $-\sigma$, in equation (76) adds nothing to the K value, K is equal to $\sigma\sqrt{\pi a}$. One can

also observe that the term, $-\sigma z$, in equation (77) adds nothing to the opening displacements along the crack line. Thus both the K value and the elliptical opening shape of the crack are the same as would be found for a central crack of length, 2a, in the presence of a remote stress field given by $\sigma_y = \sigma_x = \sigma$.

From examination of the real part of function Z_6 of reference A, at a location, $y = 0$, $x = a + r$ (where $r << a$), the corresponding value of K is given by

$$K = \frac{2P}{\pi} \frac{\sqrt{\pi a}}{\sqrt{a^2 - b^2}} \tag{78}$$

As a matter of consistency, it is clear that integration of equation (78) from $b = 0$ to $b = a$ using $P = \sigma\, db$ should give $K = \sigma\sqrt{\pi a}$. The identity:

$$\sigma\sqrt{\pi a} = \frac{2\sigma\sqrt{\pi a}}{\pi} \int_0^a \frac{db}{\sqrt{a^2 - b^2}} \tag{79}$$

is easily established by noting that

$$\int_0^a \frac{db}{\sqrt{a^2 - b^2}} = \frac{\pi}{2} \tag{80}$$

Equation (76) can be derived by means of a similar integration method applied to the function Z_6 of reference A. However, proper treatment of the complexities involved in completing this task seems inappropriate relative to the analysis level of this discussion.

Consideration will now be given to a crack problem in which the stress field local to the leading edge of the crack is modified so as to remove the stress singularity at the crack tip. The basic idea employed here was suggested by Barenblatt in 1959 and by Dugdale in 1960. Assume first that the stresses near the leading edge of an opening mode crack can be derived from equation (46) or from Z_1 of reference A

$$Z_1 = K/\sqrt{2\pi z} \qquad (46)$$

Using Z_2 of reference A we can superimpose uniform closure forces, $P = -\sigma_Y\, db$, on the crack surfaces along a segment of length, b_o, adjacent to the crack tip. This can be done using an integration of Z_2 (of reference A) from $b = 0$ to $b = b_o$. The result is a new stress function, Z_3 (of reference A) where

$$Z_3 = \frac{K}{\sqrt{2\pi z}} - \int_0^{b_o} \frac{\sigma_Y db}{\pi(z + b)} \sqrt{\frac{b}{z}} \qquad (81)$$

If we assume σ_Y is fixed from physical considerations, the final step consists in the adjustment of the sizeof b_o so that the crack tip region has no stress singularity. Integration of equation (81) is assisted by substituting $z \sin^2 u$ for the variable, b. Thus

$$db = 2z \sin u \cos u\, du$$

$$\frac{db}{z + b}\sqrt{\frac{b}{z}} = \frac{2 \sin^2 u \cos u\, du}{1 + \sin^2 u}$$

$$= 2 \cos u\, du - \frac{2 \cos u\, du}{1 + \sin^2 u}$$

$$\int_0^{b_o} \frac{db}{z + b}\sqrt{\frac{b}{z}} = 2\sqrt{\frac{b_o}{z}} - 2 \arctan \sqrt{\frac{b_o}{z}}$$

Using the above results

$$Z_3 = \frac{K}{\sqrt{2\pi z}} - \frac{2\sigma_Y}{\pi}\sqrt{\frac{b_o}{z}} + \frac{2\sigma_Y}{\pi} \arctan \sqrt{\frac{b_o}{z}} \qquad (82)$$

From equation (82) it is evident that if we choose b_o so that

$$K = \frac{2\sigma_Y}{\pi}\sqrt{2\pi b_o} \qquad (83)$$

Then the terms inversely proportional to $\sqrt{\zeta}$ cancel and

$$Z_3 = \frac{2\sigma_Y}{\pi} \arctan\sqrt{\frac{b_o}{\zeta}} \qquad (84)$$

With regard to the opening displacements near the crack tip, an equation for these can be derived from study of $\mathrm{Im}\ \bar{Z}_3$ where $\bar{Z}_3$ is as given in reference A. This requires finding the imaginary part of a complex variable function of the form

$$\arctan f = A(x,y) + i\,B(x,y) \qquad (85)$$

For those who wish to examine this detail, one can write

$$\tan f = \sqrt{\frac{b_o}{\zeta}} = \tan (A + iB) \qquad (86)$$

The real and imaginary parts of tan (A + iB) can be found. Comparisons between the real and imaginary terms of equation (86) then result in a value for B as a function of distance, r, from the crack tip along $\theta = \pi$. This discussion will skip these analysis details. The final expression for the crack line displacements, η, is, however, of interest and turns out to be as follows:
for $r \le b_o$

$$E\,\eta = \frac{4\sigma_Y}{\pi}\left\{\sqrt{b_o\, r} - (b_o - r)\arctan\sqrt{\frac{r}{b_o}}\right\} \qquad (87)$$

On $y = 0$, $\theta = 0$, $\sigma_y = (2\sigma_Y/\pi)\arctan\left(\sqrt{b_o/r}\right)$.

Thus σ_y approaches the value σ_Y as r approaches zero. Further study (again involving some analysis complexities) shows that $\sigma_y = \mathrm{Re}\ Z_3 = \sigma_Y$ on $\theta = \pi$ when r is less than b_o, and that $\mathrm{Re}Z_3 = 0$ on $\theta = \pi$ when r is greater than b_o. Examination of equation (31) shows that the assumed closure forces cause η to approach zero, as r approaches zero, in such a manner that the slope of the crack opening $(d\eta/dr)$ is zero at $r = 0$. This behavior is in contrast to the infinite value of $d\eta/dr$ (at $r = 0$) when the stress singularity is not removed and the crack tip opening has a parabolic shape.

The removal of thecrack tip singularity and modification of the crack opening shape provided by the stress function, Z_s, were of interest to Barenblatt and to Dugdale for different reasons. Barenblatt was concerned with cleavage of materials possessing well defined cleavage planes and thought some representation of bonding forces should be provided near the crack tip where the small separation of the crack surfaces might be expected to induce bonding forces. Dugdale thought of the region of length b_o, where $\sigma_y = \sigma_Y$, as an approximate representation of the influence of plastic yielding directly ahead of the crack. Thus σ_Y was regarded as a tensile yield point property of the plate material and the end point of the actual crack opening separation was considered to be at $x = - b_o$. The opening separations given by equation (87) in the region from $x = - b_o$ to $x = 0$ were regarded as representing various degrees of localized plastic stretch of the plate. Although such a model of the plastic zone at the leading edge of an actual crack is considerably over-simplified, the Dugdale or "strip" model of the plastic has proved to be useful particularly for purposes of estimating the opening stretch of the crack at the position where the actual crack and the crack tip plastic zone intersect. This aspect will be given additional discussion at a later point.

The implications suggested by the stress field corresponding to equation (84), which are of basic importance to K value characterization of cracks, are as follows. One can observe that the closure forces introduced near the crack tip are a system of self-balanced forces localized along a region of length, b_o. At distances from the crack which are large in comparison to b_o, these closure forces have little influence on the general stress pattern, and the stresses can be derived approximately from equation (46). It is also apparent that the influences of plastic or non-linear strains near the crack

tip might be represented by a wide variety of analysis model choices. The desirability of the various plausible models would changewith the ratio of plastic zone size to plate thickness as well as with the nature of the plate material. However, all such choices would have a common characteristic; each could be pictured in terms of a local system of self-balancing (or residual) stresses which would contribute very little to the stresses surrounding and well removed from the crack tip plastic zone. Considering these facts and the desirability of performing the characterization in a manner which is as nearly unpresumptive as possible, we will take the view that characterization of the stresses which control crack extension in terms of a K value is ~~most~~ appropriate for practical applications whenever the plastic or non-linear strains are confined to a region which is small in comparison to the crack size and to the net section of the component containing the crack. In this way we not only avoid presumptive assumptions pertaining to the region of plastic or non-linear strains adjacent to the crack tip but also maintain a maximum degree of analysis simplicity.

The Strip and r_Y Models of the Plastic Zone

Solutions for certain crack problems in which the plastic zone of the crack is represented by a "strip" plastic zone along the lines suggested by Dugdale (1960) are given by stress functions Z_3, Z_7, and Z_{10} of reference A. Returning to the simplest of these problems, the semi-infinite crack with a strip plastic zone, the stress σ_y was given by $\sigma_y = \sigma_Y$ for $\theta = \pi$, $r < b_o$ and by

$$\sigma_y = \frac{2\sigma_Y}{\pi} \arctan \sqrt{\frac{b_o}{r}} \qquad (83)$$

for $\theta = 0$. The value of $\arctan \sqrt{b_o/r}$ approaches $\sqrt{b_o/r}$ when r is large compared to b_o. Using equation (83), it is seen that, for $r >> b_o$, the value of σ_y is nearly given by $K/\sqrt{2\pi r}$. The value of r/b_o at which equation (88) can be nearly represented by an equation of the form

$$\sigma_y = \frac{K}{\sqrt{2\pi r_1}} \qquad (89)$$

can be substantially reduced by taking the measurement point for r to be a small distance ahead of the visual position of the crack tip. Suppose, for example, that we compare the stresses derived from equation

$$Z = \frac{2\sigma_Y}{\pi} \arctan \sqrt{\frac{b_o}{\zeta}} \qquad (84)$$

with those derived from

$$Z = \frac{K}{\sqrt{2\pi \zeta_1}} \qquad (90)$$

where the coordinate origin for ζ_1 is placed at the position $y = 0$, $x = -\frac{2}{3} b_o$. Along the positive branch of the x axis, if we insert the

approximation

$$\arctan\sqrt{\frac{b_o}{r}} = \sqrt{\frac{b_o}{r}}\left(1 - \frac{1}{3}\ \frac{b_o}{r}\right) \tag{91}$$

we find

$$\sigma_y = \frac{2\sigma_y}{\pi}\ \frac{\sqrt{2\pi b_o}}{\sqrt{2\pi r}}\ \left(1 - \frac{1}{3}\ \frac{b_o}{r}\right) \tag{92}$$

Using equation (90) and the approximation

$$\left[2\pi\left(r + \frac{2}{3}\ b_o\right)\right]^{-\frac{1}{2}} = \frac{1}{\sqrt{2\pi r}}\left(1 - \frac{1}{3}\ \frac{b_o}{r}\right) \tag{93}$$

leads to

$$\sigma_y = \frac{K}{\sqrt{2\pi r}}\ \left(1 - \frac{1}{3}\ \frac{b_o}{r}\right) \tag{94}$$

Comparison of equations (92) and (94) suggests that, if the σ_y stresses are derived from equation (90), approximate agreement with the stresses derived from equation (84) will be found at smaller values of r/b_o than would be true for other locations of the coordinate origin of the vector, ζ_1. The same location for the origin of the vector, ζ_1, is indicated also by a comparison of first approximations to the half-opening of the crack, η. Thus it can be seen that an improvement of the fit of the linear-elastic stress field to the stress field corresponding to Z_3 can be obtained by assuming the position of the crack tip, for analysis purposes, is moved forward into the plastic zone by the amount

$$\frac{b_o}{3} = \frac{\pi}{24}\left(\frac{K}{\sigma_Y}\right)^2 \tag{95}$$

A similar shift of the crack tip for analysis purposes was introduced during the period 1957-1960 (Wells, 1957; Irwin, 1960) independently of any knowledge of the strip model of the plastic zone. This is termed the r_Y model of the plastic zone and was based upon the following elementary considerations.

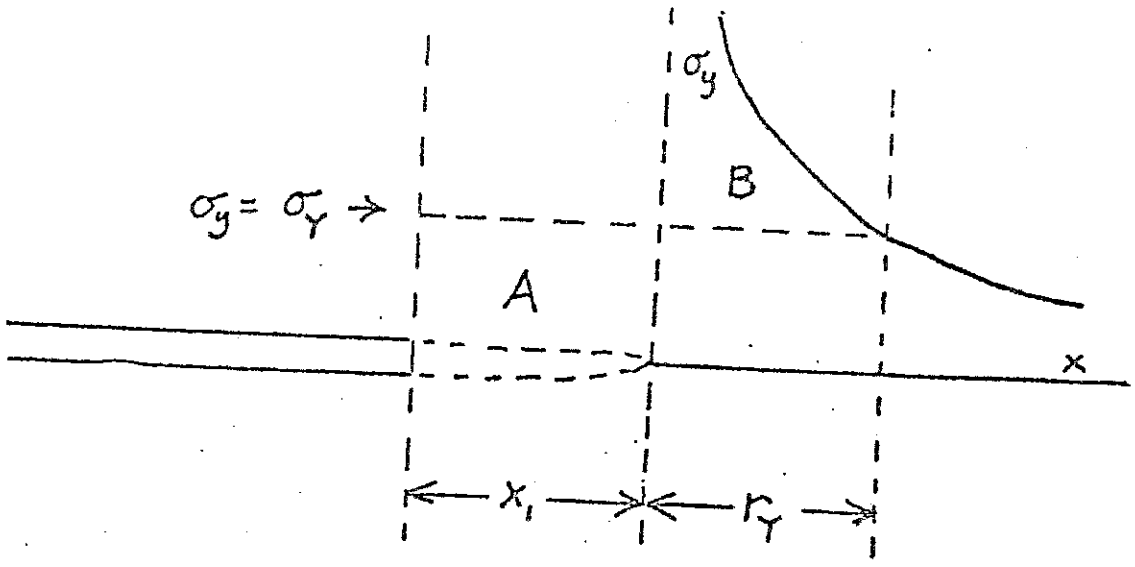

Figure 6

Assume the crack tip (foranalysis) is moved forward from the visual leading edge as shown in Figure 6, and that the distance from this new crack tip location to the position on the x axis where $\sigma_y = \sigma_Y$ is termed r_Y. From the equation

$$\sigma_y = \frac{K}{\sqrt{2\pi r}} = \sigma_Y \tag{96}$$

the value of r_Y is given by

$$r_Y = \frac{1}{2\pi}\left(\frac{K}{\sigma_Y}\right)^2 \tag{97}$$

In order to determine the value of the forward adjustment of the crack tip location relative to the leading edge of the crack, x_1, a force balance equation can be used. We assume the force across the x-axis along the length interval $(x_1 + r_Y)$ is $\sigma_y = \sigma_Y$. However, the amount of force, $x_1\sigma_Y$ (rectangle A in Figure 6), has been lost due to forward motion of the crack tip. In compensation the linear-elastic representation provides the extra force across the interval, r_Y, represented by area B of Figure 6. Clearly area A and area B should be matched. Thus the force balance equation is

$$x_1\,\sigma_Y = \int_0^{r_Y} \sigma_y\, dr - r_Y\sigma_Y \tag{98}$$

Using equation (96), the integral in equation (98) is given by

$$\int_0^{r_Y} \sigma_y dr = \frac{K}{\pi}\sqrt{2\pi r_Y} \qquad (99)$$

Using equation (97) the above result is equal to $2r_Y\sigma_Y$. Thus $x_1 = r_Y$. Comparison of equations (95) and (97) shows that both of these plasticity adjustments are proportional to $(K/\sigma_Y)^2$ and that the proportionality factors differ by less than 20 percent. In the case of a third model of the plastic zone, the Mode III elastic-(perfectly) plastic model (not discussed here), the plasticity adjustment factor suggested by analysis of a semi-infinite crack is the same as equation (97). From customary practice, the defining equation for r_Y is assumed to be equation (97).

Equation (97) contains an adjustable factor, σ_Y. It is generally recognized that, where the analysis of a crack problem is assisted by use of an r_Y plasticity adjustment, the use of engineering judgment in selection of an appropriate value for σ_Y is permissible. In the case of a crack in a plate such that the nominal plastic zone, $2r_Y$, is comparable to or larger than the plate thickness, a frequent choice for σ_Y is the uni-axial tensile yield point, σ_{YS}. However, in the case of materials which work harden rapidly with plastic strain, a larger value, say the average between σ_{YS} and the ultimate tensile strength, is sometimes used. When $2r_Y$ is small compared to the plate thickness, r_Y is elevated substantially and the choices for σ_Y which have been used range from $\sqrt{3}\,\sigma_{YS}$ to $2.1\,\sigma_{YS}$. The resulting values of r_Y are then relatively small and have little effect on the K value computation.

The uncertainties of r_Y related to choice of σ_Y can be greatly reduced in the case of fracture toughness evaluations by use of a testing practice in which the "effective" crack size is computed from the ratio of a measured displacement to the load. A discussion of this method is given at a later point.

A moderate extension of the range of applicability of the characterization factors $\mathcal{G}$ and K would be expected through use of a plasticity adjustment of the crack size as discussed above. The extension of the range of applicability suggested by actual experimental results is, however, much larger than would be anticipated even from an optimistic estimate of the expected "moderate extension". The reason for this can be understood through examination of plasticity type characterizations, such as the crack opening stretch and the J-integral, which provide characterizations directly applicable to the fracture process zone at the leading edge of the crack. These topics will be discussed in later portions of the lecture notes.

Three Dimensional Crack Problems

Complete stress field solutions are available only for a few three dimensional problems. The principal examples are: a flat circular crack subjected to a remote tensile stress normal to the crack (Sneddon, 1946; Sack, 1946), and a flat elliptical crack with a remote tensile stress normal to the crack (Green and Sneddon, 1950). The first of these two problems can be regarded as a special case of the second. These linear-elastic analysis studies showed that the opened shape of the crack was ellipsoidal. Taking the x,y,z coordinate origin at the center of the flat elliptical crack, placing the end points of the major and minor axes of the elliptical crack at $z = \pm c$ and $x = \pm a$ respectively, and using the symbol η for the y-direction crack opening displacement, the ellipsoid representing the opened crack is given by the equation

$$\left(\frac{\eta}{\eta_o}\right)^2 + \left(\frac{x}{a}\right)^2 + \left(\frac{z}{c}\right)^2 = 1 \qquad (100)$$

The maximum separation of thecrack surfaces would occur at the coordinate

origin and is equal to $2\eta_o$. When $c = a$, the crack shape is flat circular and equation (1) can be written as

$$\left(\frac{\eta}{\eta_b}\right)^2 + \left(\frac{R}{a}\right)^2 = 1 \qquad (101)$$

where $R^2 = x^2 + Z^2$. Both from physical reasoning and from the crack border stress equations given by Sneddon (1946), one can see that the leading edge stress equations correspond to a stress state of plane-strain in the limit of a close enough approach to the leading edge of the crack.

It is an interesting fact that valid expressions for $\mathcal{G}$ and K can be derived for the flat circular and flat elliptical crack problems simply from knowledge of the ellipsoidal opening shape, as represented by equations (100 and 101), and from knowledge that the crack border stress equations correspond locally to a state of plane-strain. This will be demonstrated only for the flat circular crack.

Writing equation (101) in this form

$$\eta = \frac{\eta_b}{a}\sqrt{a^2 - R^2} \qquad (102)$$

and substituting $R = a - r$ where $r << a$, provides the equation

$$\eta = \frac{\eta_b}{a}\sqrt{2ra} = \frac{\eta_o}{\sqrt{\pi a}}\sqrt{2\pi r} \qquad (103)$$

This equation can be compared to the known expression for η near the leading edge of an opening mode crack (plane-strain) which is

$$E_1\eta = \frac{2K}{\pi}\sqrt{2\pi r} \qquad (104)$$

Evidently K has the value

$$K = \frac{\pi\eta_b E_1}{2\sqrt{\pi a}} \qquad (105)$$

Thus

$$K^2 = E_1 \mathcal{G} = \frac{\pi \eta_o^2 E_1^2}{4a} \tag{106}$$

In order to find the value of η_o, note that the work necessary to close the crack, $\sigma/2$ times the crack volume, is given by

$$W = \frac{\sigma}{2} \cdot \frac{4}{3} \pi \eta_o a^2 \tag{107}$$

Assuming fixed conditions of remote stress, the total stress field energy with the crack present is $(U_o + W)$ where U_o is a fixed value representing the stress field energy prior to introduction of the crack. From previous studies the value of $\mathcal{G}$ can be obtained as the fixed load (fixed σ) derivative of $(U_o + W)$ with respect to an increment of new separational area. Assume a small expansion of the crack radius, a, so that the new separational area is $2\pi a da$. In the differentiation of W to obtain $\mathcal{G}$, it is necessary to bear in mind that, from similitude, η_o must be proportional to a. This means that

$$\frac{1}{\eta_o} \frac{d\eta_o}{da} = \frac{1}{a} \tag{108}$$

Thus $\mathcal{G}$ is given by

$$\mathcal{G} = \frac{W}{2\pi a} \left(\frac{1}{a} + \frac{2}{a} \right) = \frac{3W}{2\pi a^2}$$

$$\text{or } \mathcal{G} = \sigma \eta_o \tag{109}$$

Comparison with equation (106) shows that

$$\frac{\pi \eta_o^2 E_1}{4a} = \sigma \eta_o \tag{110}$$

Thus

$$\eta_o = \frac{4 \sigma a}{\pi E_1} \tag{111}$$

The equations for $\mathcal{G}$ and K can now be stated as

$$\mathcal{G} = \frac{4\sigma^2 a}{\pi E_1} \tag{112}$$

and

$$K = \frac{2}{\pi} \sigma \sqrt{\pi a} \tag{113}$$

In the case of the flat elliptical crack and in terms of the equation for an ellipse in its most familiar form, the value of x and z on the crack border satisfy

$$\left(\frac{x}{a}\right)^2 + \left(\frac{z}{c}\right)^2 = 1 \tag{114}$$

It was stated that c was the major semi-axis. Thus $c \geq a$. A relationship between x and z equivalent to equation (114) is

$$\left.\begin{aligned} x &= a \sin \varphi \\ z &= c \cos \varphi \end{aligned}\right\} \tag{115}$$

Although the values of φ at positions such as $z = c, x = a$, and $z = -c$ are evidently 0, $\pi/2$, and π, it should be noted that φ is a parametric angle and does not correspond to a simple angle in the plane of the crack except at the end points of the major and minor axes.

The values of $\mathcal{G}$ and K^2 vary around the border of the flat elliptical crack in the same manner as the root radius of the crack opening. Their largest and smallest values occur therefore at the end points of the minor and major axes respectively. The equations for $\mathcal{G}$ and K^2 can be derived in a manner similar to that used for the flat circular crack. However, the small inward length factor, r, must be oriented normal to the crack border and this complexity lengthens the analytical work. Only the end result will be given here.

$$E_1 \mathcal{G} = K^2 = \frac{\sigma^2 \pi a}{\left(E_k\right)^2} \sqrt{1 - k^2 \cos^2 \varphi} \tag{116}$$

In equation (116), E_k is the complete elliptic integral defined by

$$E_k = \int_0^{\pi/2} \sqrt{1 - k^2 \cos^2 u}\ du \qquad (117)$$

$$k^2 = 1 - \left(\frac{a}{c}\right)^2 \qquad (118)$$

and E_1 is given its plane-strain value, $E/(1-\nu^2)$.

For $a = c$, E_k is $\pi/2$, and equation (116) gives the same results as equations (112) and (113). In the limit as c approaches infinity, $E_k = 1$ and $\phi = \pi/2$. Thus $K = \sigma\sqrt{\pi a}$ as was found for a central crack in an infinite plate with a remote tensile stress, σ, acting normal to the crack. An equivalent physical situation corresponding to plane-strain would be found in mid-thickness regions of a plate containing a central crack with a length dimension, $2a$, which is small in comparison to the plate thickness.

For the flat circular and flat elliptical cracks discussed above, the stress state is three-dimensional and corresponds to plane-strain only as the distance from the crack border becomes very small (infinitesimal) relative to the crack size. The preceding discussion assumed $\sigma_y = \sigma$ and $\tau_{yz} = \tau_{xy} = 0$ remote from the crack. Addition of uniform extensional stresses parallel to the plane of the crack would not alter equation (116).

CRACK STRESS FIELD ANALYSIS NOTES

G. R. Irwin
Lehigh University

These notes present frequently used Westergaard type stress functions. Often the purpose for use of this type of analysis is the determination of the stress intensity factor, K, or of a displacement near a crack. When the influence of plasticity is represented in terms of "strip" yield zones, the analysis can be used to determine the value of a crack opening stretch, δ, adjacent to a "strip" plastic zone. Only Mode I applications are illustrated.

With regard to function symbols

$$Z'(z) = \frac{d}{dz} Z(z), \quad Z(z) = \frac{d}{dz} \overline{Z}(z)$$

With regard to stresses

$$\sigma_y = \text{Re } Z + y \text{ Im } Z'$$

$$\sigma_x = \text{Re } Z - y \text{ Im } Z'$$

$$\tau_{xy} = - y \text{ Re } Z'$$

With regard to displacements, v and u, for the y and x directions, assuming plane-stress,

$$Ev = 2 \text{ Im } \overline{Z} - (1 + \nu) y \text{ Re } Z$$

$$Eu = (1 - \nu) \text{ Re } \overline{Z} - (1 + \nu) y \text{ Im } Z$$

Following the list of stress functions for two-dimensional problems, equations are given pertaining to a flat-elliptical crack subjected to tension normal to the crack.

1. Semi-infinite crack on y = 0 from x = 0 to x = $-\infty$.

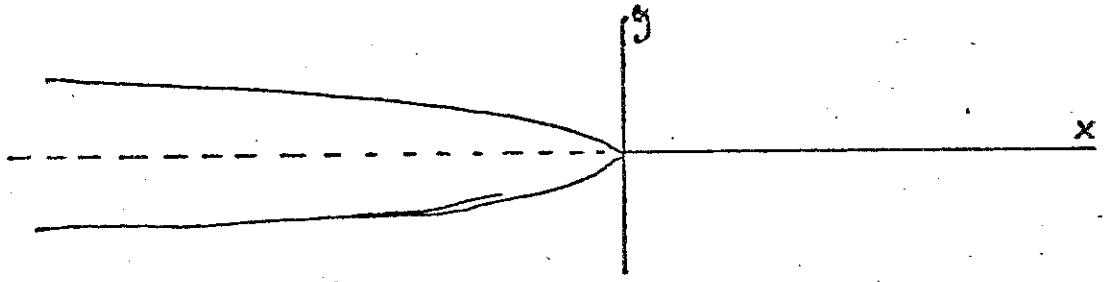

$$Z_1(z) = \frac{K}{\sqrt{2\pi z}} \quad , \quad \bar{Z}_1 = \frac{K}{\pi}\sqrt{2\pi z}$$

2. Same as (1) with pair of splitting forces of strength P (per unit thickness) acting at x = -b.

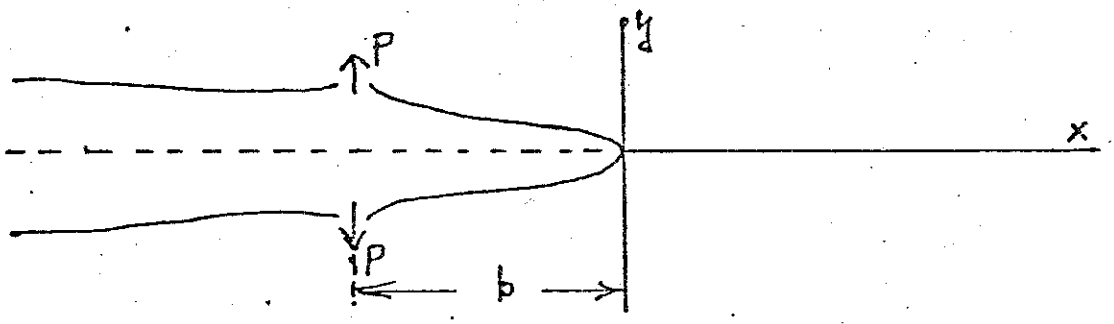

$$Z_2(z,b) = \frac{P}{\pi b}\,\frac{\sqrt{b/z}}{1+z/b} \quad , \quad \bar{Z}_2 = \frac{2P}{\pi}\arctan\sqrt{\frac{z}{b}}$$

3. Same of (1) but with a "strip" yield zone from x = $-b_o$ to x = 0.

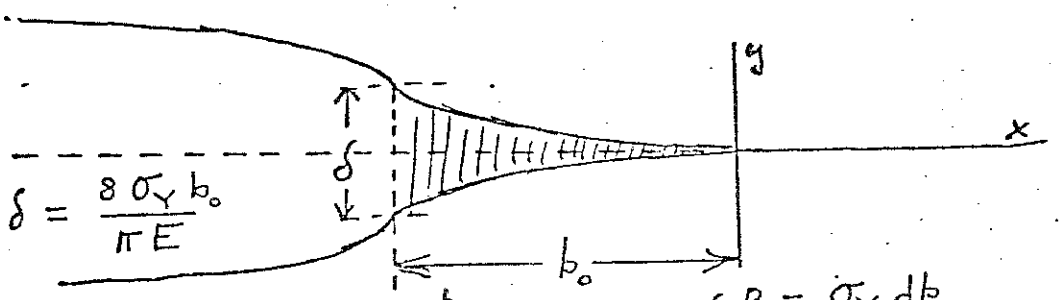

$$Z_3(z,b_o) = \frac{K}{\sqrt{2\pi z}} - \int_0^{b_o} Z_2 \quad \text{where} \quad \begin{cases} P = \sigma_Y\, db \\ K = \frac{2\sigma_Y}{\pi}\sqrt{2\pi b_o} \end{cases}$$

$$Z_3 = \frac{2\sigma_Y}{\pi}\arctan\sqrt{\frac{b_o}{z}}$$

$$\bar{Z}_3 = \frac{2\sigma_Y}{\pi}\left\{\sqrt{b_o z} - b_o \arctan\sqrt{\frac{z}{b_o}} + z\arctan\sqrt{\frac{b_o}{z}}\right\}$$

4. Central crack of length $2a$ in an infinite plate. Remote tensile stress is $\sigma_y = \sigma_x = \sigma$.

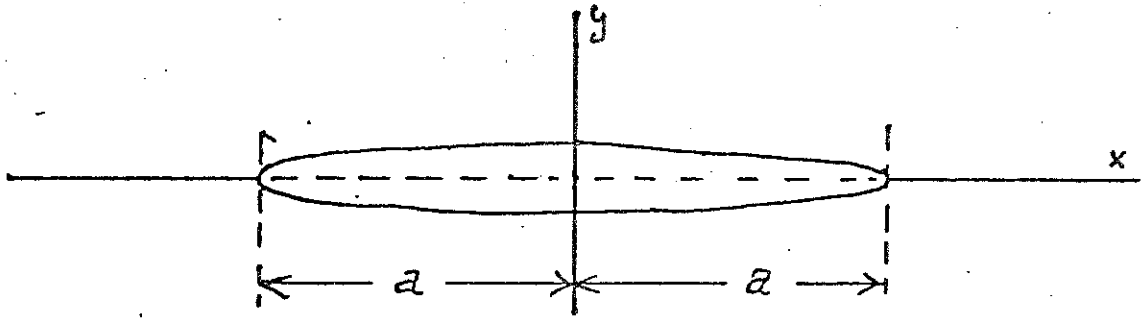

$$Z_4(z,a) = \frac{\sigma}{\sqrt{1-(a/z)^2}} \quad , \quad \bar{Z}_4 = \sigma\sqrt{z^2-a^2}$$

$$K = \sigma\sqrt{\pi a}$$

5. Same as (4) with a pair of splitting forces of strength p (per unit thickness) at x = b. Remote stresses are zero.

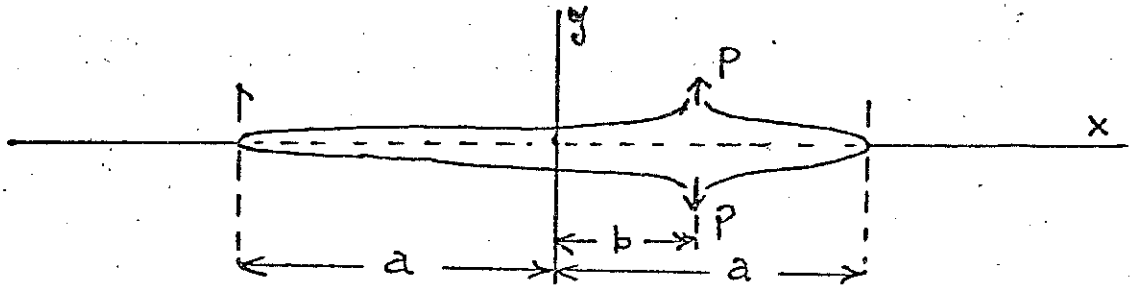

$$Z_5(z,a,b) = \frac{P\sqrt{a^2-b^2}}{\pi z(z-b)\sqrt{1-(a/z)^2}}$$

$$\bar{Z}_5 = \frac{P}{\pi}\left[\arctan\left\{\frac{\sqrt{z^2-a^2}}{\sqrt{a^2-b^2}}\right\} + \arctan\left\{\frac{b}{z}\frac{\sqrt{z^2-a^2}}{\sqrt{a^2-b^2}}\right\}\right]$$

6. Same as (5) with an additional and equal pair of splitting forces at x = - b.

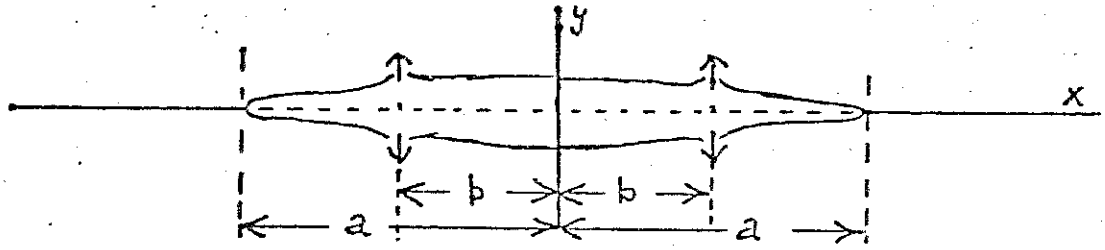

$$Z_6(z,a,b) = \frac{2P\sqrt{a^2-b^2}}{\pi(z^2-b^2)\sqrt{1-(a/z)^2}}$$

$$\bar{Z}_6 = \frac{2P}{\pi}\arctan\left\{\frac{z^2-a^2}{a^2-b^2}\right\}^{1/2}$$

7. Central crack as in (4) having "strip" yield zones at each crack end from $x = a$ to $x = c$ and from $x = -a$ to $x = -c$.

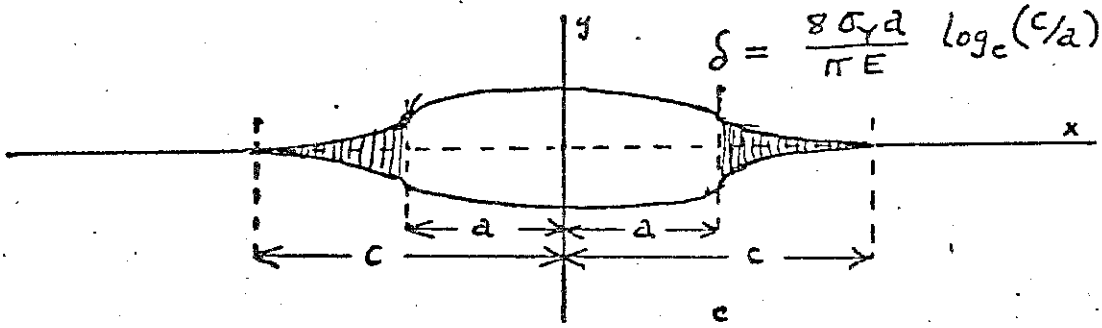

$$\delta = \frac{8\sigma_Y a}{\pi E} \log_e(c/a)$$

$$Z_7(z, a, c-a) = Z_4(z,c) - \int_a^c Z_c(z, c, b)$$

where $\begin{cases} P' = \sigma_Y \, db \\ \sigma = \frac{2\sigma_Y}{\pi} \operatorname{arcsec}(c/a) \end{cases}$

$$Z_7 = \frac{2\sigma_Y}{\pi} \arctan\left\{\frac{(c/a)^2 - 1}{1-(c/z)^2}\right\}^{1/2}$$

$$\bar{Z}_7 = \frac{2\sigma_Y}{\pi}\left[z \arctan\left\{\frac{(c/a)^2-1}{1-(c/z)^2}\right\}^{1/2} + a \arctan\left\{\frac{(z/c)^2-1}{1-(z/c)^2}\right\}^{1/2}\right]$$

8. Periodic co-linear cracks of length $2a$, the distance between crack centers being W. Remote tensile stress of $\sigma_y = \sigma_\infty$. All cracks on $y = 0$.

$$Z_8(z, a, W) = \frac{\sigma}{\sqrt{1-\left(\frac{\sin\frac{\pi a}{W}}{\sin\frac{\pi z}{W}}\right)^2}}$$

$$\bar{Z}_8 = \frac{\sigma W}{\pi} \arccos\left\{\frac{\cos\frac{\pi z}{W}}{\cos\frac{\pi a}{W}}\right\}$$

$$K = \sigma\left\{W \tan\frac{\pi a}{W}\right\}^{1/2}$$

9. Same crack pattern as (8). Remote stresses zero. Pairs of splitting forces of strength P (per unit thickness) symmetrically placed at x-separations of ± b from the center of each crack.

$$Z_9(z,a,b,W) = \frac{2P\cos\frac{\pi b}{W}\left\{\left(\sin\frac{\pi a}{W}\right)^2-\left(\sin\frac{\pi b}{W}\right)^2\right\}^{1/2}}{W\left\{\left(\sin\frac{\pi z}{W}\right)^2-\left(\sin\frac{\pi b}{W}\right)^2\right\}\left\{1-\left(\frac{\sin\frac{\pi a}{W}}{\sin\frac{\pi z}{W}}\right)^2\right\}^{1/2}}$$

$$\bar{Z}_9 = -\frac{2P}{\pi}\arctan\left\{\frac{1-\left(\frac{\cos\frac{\pi a}{W}}{\cos\frac{\pi b}{W}}\right)^2}{\left(\frac{\cos\frac{\pi a}{W}}{\cos\frac{\pi z}{W}}\right)^2-1}\right\}^{1/2}$$

10. Periodic co-linear cracks as in (8) but with "strip" yield zones of length (c - a) at each crack end.

$$Z_{10}(z,a,c-a,W) = Z_8(z,c,W) - \int_a^c Z_9(z,c,b,W)$$

where $\begin{cases} P = \sigma_Y\, db \\ \sigma = \frac{2\sigma_Y}{\pi}\operatorname{arcsec}\left(\frac{\sin\frac{\pi c}{W}}{\sin\frac{\pi a}{W}}\right) \end{cases}$

$$Z_{10} = \frac{2\sigma_Y}{\pi}\arctan\left\{\frac{\left(\frac{\sin\frac{\pi c}{W}}{\sin\frac{\pi a}{W}}\right)^2-1}{1-\left(\frac{\sin\frac{\pi c}{W}}{\sin\frac{\pi z}{W}}\right)^2}\right\}^{1/2}$$

$$\operatorname{Im}_{\text{at } x=a}\left(\bar{Z}_{10}\right) = -\int_a^c \operatorname{Im}\left\{Z_{10}(x,a,c-a,W)\right\}\,dx$$

$$\delta = \frac{4}{E}\operatorname{Im}_{\text{at } x=a}\left(\bar{Z}_{10}\right)$$

11. Stress intensity factor for a two-dimensional crack of length, a, at a free surface boundary. The remote stress normal to the crack and parallel to the free boundary is σ.

$$K = 1.12 \ \sigma \sqrt{\pi a}$$

12. Flat-Elliptical Crack

For a flat elliptical crack in an infinite solid subjected to uniform normal pressure, σ, on the crack surfaces, the Sneddon-Green stress analysis solution assumes that the displacements, u, v, w, in the x, y, z directions satisfy the equations

$$u = (1 - 2\nu) \frac{\partial U}{\partial x} + y \frac{\partial^2 U}{\partial x \, \partial y}$$

$$v = -2(1 - \nu) \frac{\partial U}{\partial y} + y \frac{\partial^2 U}{\partial y^2}$$

$$w = (1 - 2\nu) \frac{\partial U}{\partial z} + y \frac{\partial^2 U}{\partial z \, \partial y}$$

where U and $\frac{\partial U}{\partial y}$ are both three-dimensional potential functions. Values of σ_y and v can be derived from the following relations which complete the formal solution of the problem.

$$\frac{\partial U}{\partial y} = - \frac{c \, a \, \eta_o}{4(1 - \nu)} y \int_{\lambda}^{\infty} \frac{ds}{s \left[s(a^2 + s)(c^2 + s) \right]^{1/2}}$$

The boundary of the crack is given by

$$y = 0$$

$$x = a \sin \phi$$

$$z = c \cos \phi$$

Fixed values of λ correspond to closed ellipsoidal surfaces defined by the equation

$$\frac{x^2}{a^2 + \lambda} + \frac{y^2}{\lambda} + \frac{z^2}{c^2 + \lambda} = 1$$

As λ approaches zero the ellipsoidal surface tends to coincide with the upper and lower surfaces of the flat-elliptical crack. The maximum opening of the crack at its center is $2\,\eta_o$ where

$$\eta_o = \frac{2(1-\nu^2)}{E}\,\frac{\sigma\, a}{E_k}$$

E_k is the complete integral function

$$E_k = \int_0^{\pi/2} \left(1 - k^2 \cos^2 u\right)^{1/2} du$$

and

$$k^2 = \frac{c^2 - a^2}{c^2}$$

From examination of the crack opening near the boundary of the crack,

$$K^2 = \frac{\sigma^2\, \pi\, a}{E_k^2}\left(\sin^2 \phi + \frac{a^2}{c^2}\cos^2\phi\right)^{1/2}$$

At $\phi = \frac{\pi}{2}$, as k approaches unity, K approaches the known two-dimensional answer,

$$\sigma\sqrt{\pi\, a}$$

As k approaches zero, the crack shape becomes flat-circular and K is given by

$$K = \frac{2}{\pi}\,\sigma\sqrt{\pi\, a}$$

in agreement with analyses by Sneddon and by Sack published in 1946. Since K values are not altered by addition of a uniform stress field, the K values noted above can be regarded as correct for a pressure of $(\sigma - \sigma_1)$ acting on the crack surfaces and a remote normal stress, $\sigma_y = \sigma_1$.

13. Part-Through Cracks

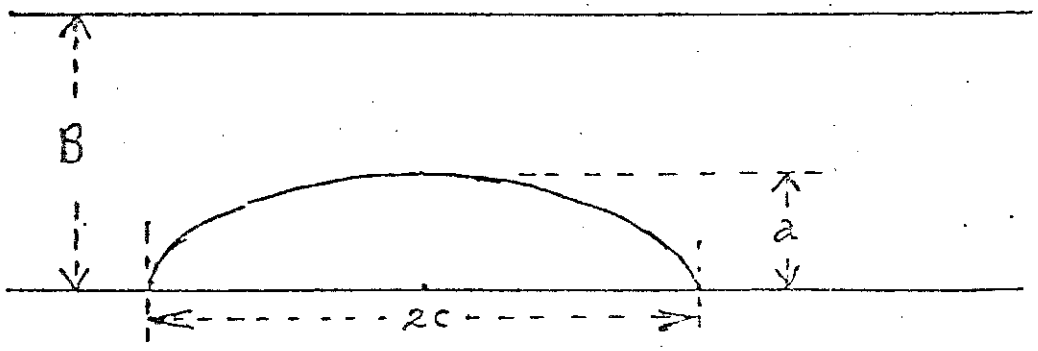

For a surface crack of depth, a, as shown, the value of K tending to cause deepening of the crack is often estimated using the equation

$$K^2 = \frac{1.2\ \sigma^2\ \pi\ a}{E_k^{\ 2} - 0.212\left(\frac{\sigma}{\sigma_{YS}}\right)^2}\ F$$

The factor, 1.2, was introduced as an allowance for the free surface influence. For F = 1, the second term in the denominator can be derived from

$$K^2 = \frac{1.2\ \sigma^2\ \pi(a + r_Y)}{E_k^{\ 2}}$$

and by assuming σ_Y is elevated by the applicable degree of plane-strain constraint to 1.68 times the uni-axial tensile yield point, σ_{YS}.

The factor F is introduced as a correction for the influence of a finite plate thickness, B. Although this subject has received study, there is no generally accepted procedure for calculation of F. The writer prefers to follow the practice of P. C. Paris in using

$$F = \frac{2\ B}{\pi\ a} \tan \frac{\pi\ a}{2\ B}$$

uniformly when the crack depth is larger than B/3. When

$$\frac{2\ c}{B - a} > 4 \text{ and } \sigma\left(\frac{B}{B - a}\right) > 1.5\ \sigma_{YS},$$

methods of analysis should be considered which take account of yielding across the net section.

Numerical Calculations of K Values

Consider first the problem of a through-the-thickness crack of length, a, extending inward normal to the free edge of a large plate and subjected to a remote tensile stress, σ, normal to the crack. This problem is pictured in Figure 1.

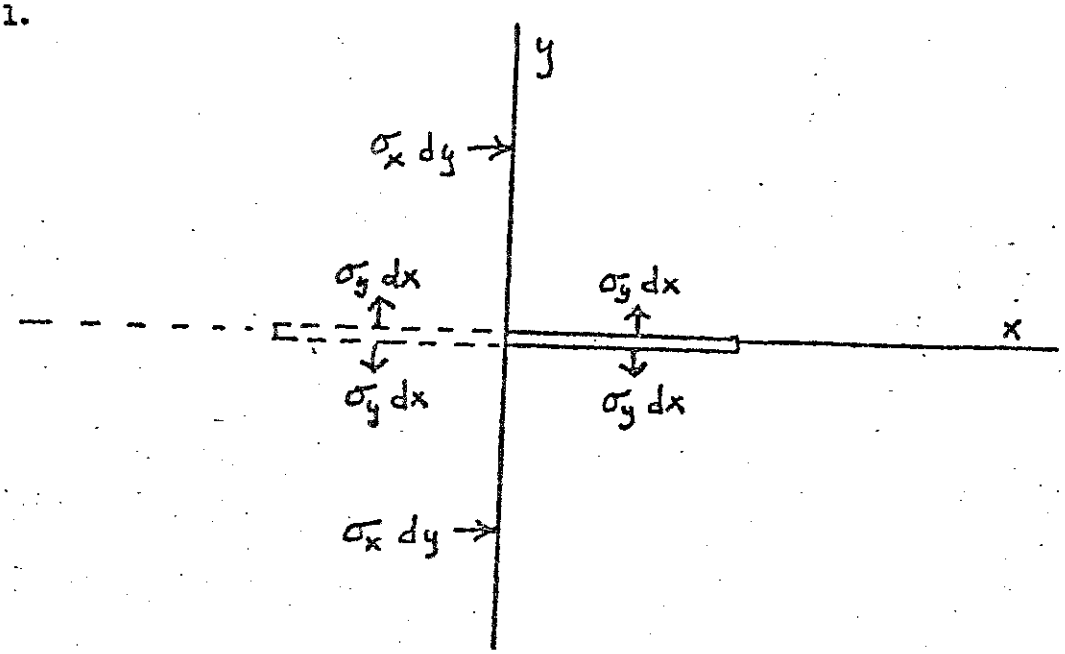

Figure 1

An appropriate numerical method for obtaining the K value for the crack problem is one of successive approximation. Since the K value does not depend upon whether σ is applied as a remote tensile stress or as a pressure in the crack, it is convenient to start with the latter viewpoint. The first approximation of K then becomes $K_1 = \sigma\sqrt{\pi a}$. In order to obtain a second approximation, the stress function

$$Z = \frac{\sigma}{\sqrt{1-(a/z)^2}} - \sigma \qquad (1)$$

is used to compute the values of σ_x and τ_{xy} on $x = 0$. These must be removed because the line $x = 0$ is a free edge of the plate. Because of the symmetry of the above stress function, τ_{xy} is zero on $x = 0$ and only the stresses, σ_x, need to be removed. This is done by adding a stress field consisting of pressure forces, $\sigma_x dy$, along the line $x = 0$, as shown in the figure. Superposition

of this stress field adds nothing to the K value. However, it does place unwanted tensile stresses, σ_y, across the line of the crack. These are a function of the pressures, $\sigma_x d_y$, integrated along the line, x = 0, and must be tabulated in preparation for the second step of the calculation.

The second step consists in removal of the unwanted tensions σ_y dx on the crack line by application of equal pressure forces as shown in Figure 1. It is best to apply these forces in a symmetrical manner relative to the y-axis in order to avoid applying unwanted shearing stress, τ_{xy}, on the line, x = 0. Two results are needed. One of these is the second approximation to the K value using the equation

$$K_2 = K_1 + \int_0^a \frac{2\sigma_y \, dx}{\pi\sqrt{a^2-x^2}} \qquad (2)$$

The second result needed is a new tabulation of the unwanted pressures, σ_x dy, along the line, x = 0, caused by application of the pressures, σ_y dx, in the crack. These can be computed using the stress function

$$Z = \int_0^a \frac{2\sigma_y \, dx}{\pi(z^2-x^2)} \; \frac{\sqrt{a^2-x^2}}{\sqrt{1-(a/z)^2}} \qquad (3)$$

The procedures for obtaining third and fourth approximations to the K value are simply repetitions of the second step as discussed above. In the required tabulations, choices must be made of finite intervals and positions for the force application within each interval. Along the line, x = 0, it is helpful to substitute y = a tan u_1 and use equal intervals in terms of the angle variable u_1. Such a choice recognized the diminishing importance of an applied pressure, σ_x dy, with increase of y. For similar reasons, on the line, y = 0, it is helpful to substitute x = a sin u_2 and use equal intervals in terms of the angle variable u_2.

The calculation described above converges rapidly and is conservative with regard to use of computor time. In compensation a considerable computor programming effort is required. The latter can, however, be substantially reduced through careful study of the equations. In the case of the problem of Figure 1, the answer obtained is

$$K = 1.122\,\sigma\sqrt{\pi a} \qquad (4)$$

The correction factor for the influence of the free surface is believed to be accurate to 0.[illegible] percent.

Consider next the calculation method termed "boundary collocation". This method is most clearly appropriate for problems such as those shown in Figure 2.

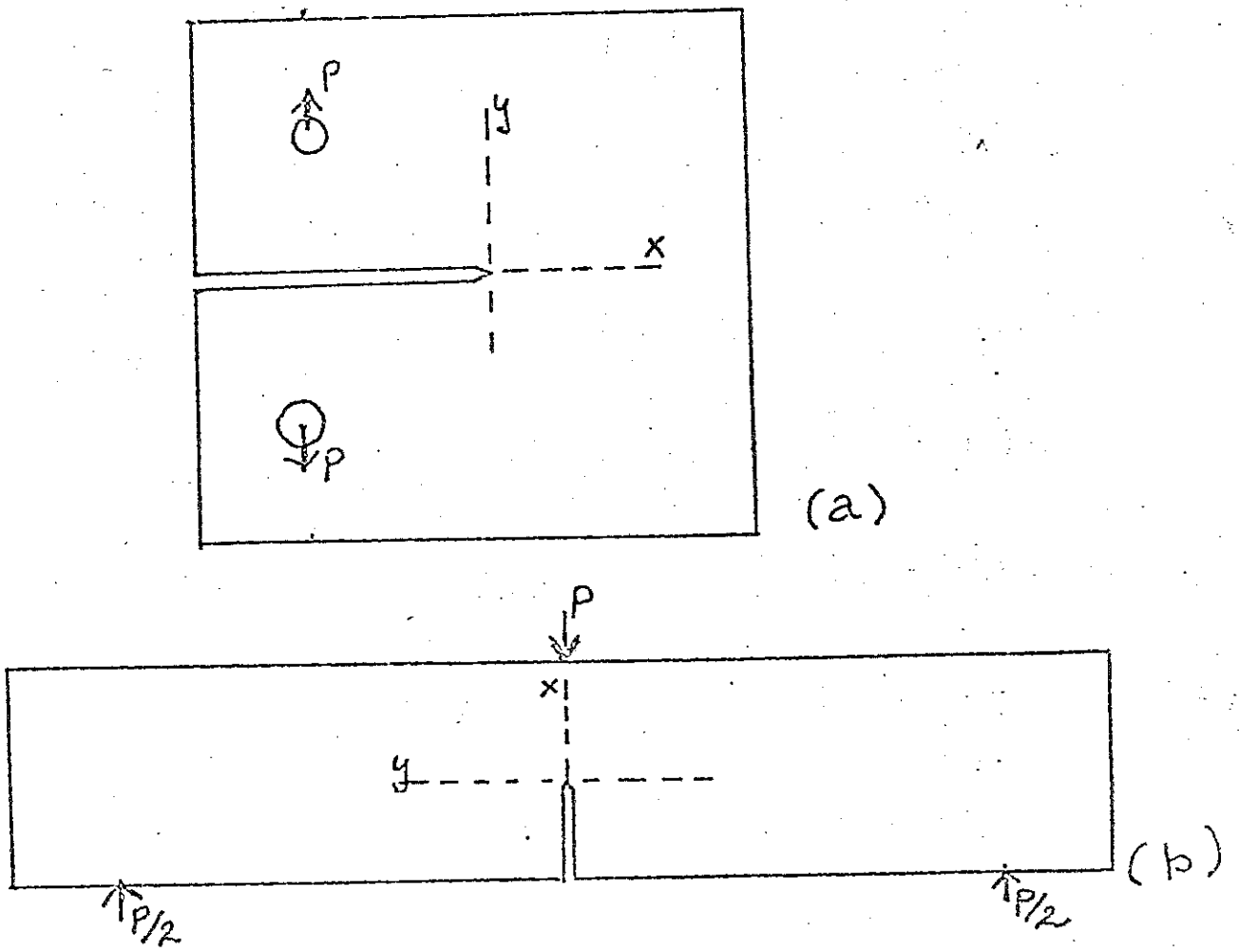

Figure 2. (a) A compact tension test specimen
(b) a notched-bend test specimen with 3-point loading

The basic relationship used in this method is the Westergaard stress function

$$Z = \frac{K}{\sqrt{2\pi\zeta}} + A_1\left(\frac{\zeta}{a}\right)^{\frac{1}{2}} + A_2\left(\frac{\zeta}{a}\right)^{3/2} + \cdots + A_m\left(\frac{\zeta}{a}\right)^{m-\frac{1}{2}} \qquad (5)$$

where the coordinate origin is regarded as located at the crack tip and the constants A_1, A_2, etc. are all real and have the dimensions of stress. Note that the exponent of each term on the right of equation (5) is such that its real part is zero along the negative branch of the x-axis. Thus, if the coordinate directions are selected as shown in Figure 2, the form of equation (5) supplies a proper stress condition near the crack tip and maintains $\sigma_y = \tau_{xy} = 0$ along the crack line.

The term, boundary collocation, implies that the (m+1) constants of equation (5) will be adjusted so as to satisfy boundary conditions at a selected group of boundary points. In general two stresses, the normal stress and the shear stress(parallel to the boundary) are known at each selected boundary point. Thus a selection of $\frac{m+1}{2}$ boundary points would provide (m+1) equations, enough to determine the constants in equation (5). Experience with calculations of this kind has indicated that it is best to limit the value of m, choose (m+1) or more boundary points and evaluate the constants of equation (5) using a "least squares" program. Where the problem implies application of a force at a point fairly close to the crack tip, judgment must be used in the selection of boundary points and boundary stress conditions so that the influence of the concentrated load is adequately represented.

If the only result needed from the calculation is the value of K, a tabulation of values for the remaining constants of equation (5) would be unnecessary. The goal of the calculation would then be to find the proportionality of K to the applied load for a series of crack size values across the

range which is of interest for testing purposes. The results for a specimen similar to (a) of Figure 2 are given in ASTM test method E-399. The results for several specimens similar to (b) of Figure 2 are given in ASTM STP 381.

Wells + Post - Proc. SESA 1958, vol. p ?.
Clark & Irwin, Experimental Mechanics, 1966.

CRACK EXTENSION BEHAVIOR PATTERNS

The crack extension process is associated with growth and joining of advance origins and this tends to be discontinuous at fine scale. The speed of a real crack can therefore, be defined and measured only as the average time rate of displacement of the apparent leading edge across distances much larger than the size of the small discontinuous units of separation. In the case of nearly plane-strain conditions at the leading edge, estimating the size of the largest discontinuous units at $0.5\ r_Y$ seems reasonable. The concept of movement of the leading edge involves averaging across such irregularities parallel to the leading edge as well as in a forward direction. Possibly $2r_Y$, the nominal plastic zone size, would therefore represent a fair guess at the smallest forward advance of the leading edge across which an average crack speed determination can be regarded as significant in consideration of small scale irregularities.

Although exceptions can always be found, the behaviors termed onset of rapid fracturing and crack arrest are relatively abrupt in the sense that they tend to occur within a forward extension increment smaller in size than $2r_Y$. When, for purposes of simplicity we adopt a terminology based upon linear elastic stress analysis to discuss crack extension behaviors, the analysis regards length dimensions of size r_Y or $2r_Y$ as infinitesimals. Therefore, both in consistency with the analysis basic to definition of K and $\mathcal{G}$ and in consistency with the averaging process implicit in definition of crack speed, the customary behavior of real cracks under rather brittle conditions suggests that onset and arrest of rapid fracturing occur with essentially perfect abruptness. That is to say, for reference purposes, the ideal concept of onset of rapid fracturing is an abrupt increase of crack speed from a very small or zero value to a much larger magnitude. Correspondingly crack arrest is an abrupt drop of the crack speed to a very small or zero value from a velocity of substantial magnitude.

Observations have shown that when the value of $\mathcal{G}$ is large enough to maintain rapid crack extension, the fracturing process is stable in the sense that a fixed $\mathcal{G}$ produces a fixed crack speed. Continued increase of $\mathcal{G}$ moves the crack extension behavior into a maximum velocity regime in which a substantial, say 20 percent, increase of $\mathcal{G}$ causes negligible increase of the crack speed. The maximum velocity regime terminates with development of the abrupt instability termed crack division (for a long through-crack in a plate) or hackel (for a deeply embedded brittle crack).

Stress analysis aspects of rapidly moving cracks are somewhat incomplete. Problems in which the crack speed is constant or changes only a few percent across increments of extension of, say 20 r_Y, can be solved at least in terms of complete statements of the necessary computational procedure. On the other hand, for periods in which the acceleration or deceleration is too large for such a viewpoint, basic analysis questions exist which need further study. However, it seems probable experiments will not distinguish in a clear way between effects due to rapid velocity changes and those due the inherent small scale discontinuities of cracking which must be covered in any case by the concept of an average crack speed. The following comments based upon the steady or slow changing crack speed idea may therefore be of interest.

A stress distribution was published by Yoffe* for a two-dimensional crack of constant length 2a moving at a fixed crack speed in an infinite solid with the tension σ acting normal to the crack at infinity. The value of K for the leading edge of this crack was $\sigma\sqrt{\pi a}$, the same as for the similar static problem. Since Yoffe's analysis was based on crack-closure action proceeding at the same speed

---

* E. H. Yoffe, Phil. Mag. Vol. 42, p. 739, 1951.

as the opening process, the usefulness of this solution was not at first clear. However, the prediction from Yoffe's analysis, that the limit to the speed of a crack fixed by inertia is the Rayleigh wave velocity, is generally correct. A stable crack speed higher than this would not be possible because a fixed pattern of crack-opening displacements could not then advance as fast as the leading edge of the crack. Thus, the limiting velocity of a brittle crack from purely inertial limitations is about $0.9c_2$, where c_2 is the elastic shear-wave speed.

Such analytical study as has been given to practical dynamic-fracturing problems, for example, crack arrest studies in large welded test plates, has been of the static kind. There is some evidence from data consistency that errors from not using a dynamic treatment have been relatively small. For the running crack, the inertia of surrounding plate material delays interaction of the crack-tip stress field with the points of load application and specimen boundaries. The expected effect of this delay is a reduction of the K value below the static estimate. Essentially the plate material inertia provides a short-specimen fixed-grip condition to a partial degree. However, for small crack speeds, the dynamic effect influencing an estimate of K should be small.

The available information suggests that static methods of analysis are serviceable for purposes of estimating the crack arrest possibilities in a compact structure, for example, a rectangular test plate or a thick-walled pressure vessel. In the case of more compliant structures, a static analysis would usually be conservative but study should be given to stress wave reflections capable of producing tension across an arrested crack.

Assisted by the use of ultra-sonic ripple markings, crack speed behaviors in a number of glasses have been studied in considerable detail. * A close

* H. Schardin, D. Elle, and W. Struth, Z. Tech. Physik. Vol. 21, p. 393, 1940.

approach to the Rayleigh wave velocity was never observed. The maximum crack speed in common soda-lime glass was not far from half the shear wave speed, c_2. However, a correlation with internal damping was found. For example, a maximum crack speed of about $0.6c_2$ was noted in nearly pure silica glass and maximum speeds smaller by more than a factor of two occurred in several glasses containing lead.

Crack division depends upon attainment of a maximum speed. This can be understood in terms of the relationship of crack speed ($\dot{a}$) to the value of $\mathcal{G}$. When $da/d\mathcal{G}$ is large, small preliminary efforts at crack division do not succeed because the $\mathcal{G}$ values for each of the competing new branches are unlikely to be equal. A small $\mathcal{G}$ value difference would give a large crack speed advantage to the highest $\mathcal{G}$ branch. Thus, the largest branch-crack stress relieves and stops its competitors. On the other hand, after attainment of limiting velocity where $da/d\mathcal{G} = 0$, the crack speed disadvantage of the shorter of several competing new branches is much less, and successful crack division soon develops.

In summary, from examination of the crack speed in relation to the force $\mathcal{G}$, one finds that for relatively brittle solids, a running tensile crack is essentially an overdamped, low-inertia disturbance which cannot be driven faster than about half the elastic-shear-wave velocity. The regime, in which the crack speed adjusts to a stable balance between the energy-dissipation rate and the driving force $\mathcal{G}$, is bordered at the high end by the limiting crack speed and the unstable behaviors termed crack division and hackle. At the low end of the regime, there is a minimum stable crack speed and the unstable behaviors termed crack arrest and onset of rapid fracture. Characterization of these low-speed instability behaviors in terms of critical values of $\mathcal{G}$ or K receives considerable use in crack-toughness testing. When the test material is strain-rate sensitive, the low-speed instability behaviors tend to become more abrupt and also more complex in the sense that onset of rapid fracture typically requires a larger stress factor K than is required for crack arrest.

THE R-CURVE APPROACH TO FRACTURE CHARACTERIZATION

by

G. R. Irwin
Lehigh University

In order to give linear elastic fracture mechanics an extended range of applicability, it is helpful to correct (or adjust) the crack size for the influence of the plastic zone associated with each leading edge. For this purpose we can add r_Y at each crack tip where

$$r_Y = \frac{1}{2\pi}\left(K/\sigma_Y\right)^2 \qquad \text{-------(1)}$$

and σ_Y is the yield point stress.

Consider next the Griffith crack equation

$$E\mathcal{G} = K^2 = \pi\sigma^2(a + r_Y) \qquad \text{-----(2)}$$

$$\text{From Eq. (1)} \quad K^2 = \frac{\pi\sigma^2 a}{1 - \frac{1}{2}(\sigma/\sigma_Y)^2} \qquad \text{---------(3)}$$

$$\text{and} \quad r_Y = \frac{\frac{1}{2}(\sigma/\sigma_Y)^2 a}{1 - \frac{1}{2}(\sigma/\sigma_Y)^2} \qquad \text{---------(4)}$$

We would like to believe all crack-like flaws in our structures are small enough so that the applied tensile load σ can be nearly as large as σ_Y. From Equation (4) one can see this means r_Y cannot be negligible in comparison to the half-length of the crack, a. On the other hand, the characterization factors, K and $\mathcal{G}$, can be given an exact interpretation as stress field parameters only in the limit as the nominal plastic zone size, $2\,r_Y$, becomes infinitesimal relative to the dimensions of the crack and of the net section.

Consider next the determination of a toughness characterization, K_c (or $\mathcal{G}_c$), pertaining to onset of rapid fracturing. It has been observed that when the crack simulating notch is "sharpened" by a segment of low-amplitude fatigue cracking, a slow-stable crack extension

comparable in size to 2 r_y often precedes onset of rapid fracturing. The lack of abruptness of the instability point thus introduced leads to a corresponding uncertainty in the K_c determination. The degree of this uncertainty would, of course, be unimportant if 2 r_y was truly infinitesimal in relative terms. However, the size of samples available for testing as well as economy sometimes persuades us to conduct the fracture tests with specimens such that 2 r_y is not negligible in comparison to the crack and net section dimensions. In addition we know that test results pertaining to values of 2 r_y comparable to the crack size do have practical interest as illustrated in the opening comments.

For the reasons discussed above it is desirable to consider next a method for characterization of crack toughness which retains model type applicability to cracks in real structures even when the nominal plastic zone size is not small in comparison to the size of the crack.

For a through-the-thickness crack in a plate during slow-stable crack extension we can define the resistance to crack extension, R, as the value of the tensile driving force $\mathcal{G}$ required to cause each additional increment of stable crack extension. Results of R-curve measurements generally similar to the solid curve in Fig. 1 have been obtained by Heyer and McCabe[4]. The effective crack size, a_e, is $a_e = a_o + a_s + r_{YS}$ where a_o is the crack size prior to loading and a_s is the amount of slow-stable extension.

Examinations of R-curve measurements for a variety of high strength metal sheets in which the notch "sharpening" employed low-amplitude fatigue suggest that a_s is usually about 2 r_{YS} when the resistance reaches 95 percent of the plateau value.

For specific illustration, we can assume Fig. 1 represents R-curve test results obtained using the specimen shown in Fig. 2. Separational loads, we assume were applied by wedge action in the central hole in order to avoid onset of rapid fracturing prior to reaching the plateau portion of the R-curve. During increase of the separational load, the increase of effective crack size consists at first only in the growth of r_Y. Most of the slow-stable extension termed a_s occurs during the final 20 percent of load increase.

The initial shape of the leading edge of the crack, which we assume was established by low-amplitude fatigue, would be nearly straight across the plate-thickness, and the fracture surfaces adjacent to the leading edge would be relatively smooth. When the $\mathcal{J}$ value becomes large enough to produce forward motion of the crack, additional increase of R is assisted by the tendencies toward development of shear lips, toward a shape change of the leading edge, and toward more and more irregularity in flat-tensile regions of the fracture.

We assume next that, if the initial crack of Fig. 1 had been caused to extend by remotely applied tensile loading, then the development of resistance to crack extension as a function of effective crack size would have been the same as the R-curve obtained using wedge loading. The two dashed curves on Fig. 1 represent $\mathcal{J}$ as a function a_e for two fixed values of the remote tensile stress, σ. When σ is small, one can see that increase of a_e with σ fixed causes an increase of $\mathcal{J}$ which is much smaller than the increase of R. Therefore the crack is stable. When σ is large enough so that the corresponding dashed curve is just tangent to the R-curve, the increase of $\mathcal{J}$ provided by increase of a_e (with σ fixed) is equal to or larger than the corresponding increase of R. When a_e has increased to this tangency point, onset of rapid fracturing can be expected to occur.

When a centrally notched plate is loaded to fracture in an actual testing machine, fixed load conditions are rarely maintained. Thus a small reduction of the load, assisted by irregularities in the resistance to crack extension, may increase the observed slow-stable extension of the crack beyond the amount one might predict from examination of the R-curve. Thus a considerable uncertainty may exist as to the particular value of a_e which should be used, along with the observed critical value of the load, in calculations of $\mathcal{G}_c$ (and K_c). One must, however, bear in mind that the critical value of the remote tensile load and the value of the initial crack size are both determined with negligible ambiguity in the R-curve experiment. Since the object of the toughness investigation is to permit determinations of critical tensile loads for various initial cracks, we should not be distressed if we find it is possible to accomplish this task more conveniently through determination and study of the R-curve than through determination of $\mathcal{G}_c$.

Added generality in use of R-curve measurements is at hand if we assume the change of shape of the R-curve with increase or decrease of initial crack size is negligible. Although there are some uncertainties pertaining to the assumptions, basic to the R-curve approach, it is believed these can be accepted with little risk of significant error so long as the loads remain below those necessary for general yielding. The R-curve shape can, of course, be expected to change with change of the plate thickness.

R-curve measurements can be assisted by using observations of the crack opening to determine the effective crack size. For example, in the case of a single-edge-notched (SEN) specimen, a clip-gage can be employed at the free edge of the specimen where the notch has its largest opening displacement. From prior calibration, we know the ratio of

crack opening displacement to applied tensile load for each crack size, assuming linear response and negligible plastic strain. It can also be assumed that the ratio of opening displacement to load when a visible indication of non-linear response is present, provides as good a measure of a_e as would be obtained through addition of r_Y to the directly observed crack size. In fact, for some alloys which strain age at room temperature (e.i. 2024-T351 aluminum), it is difficult to guess what value of σ_Y should be used in computing r_Y, and use of the value of a_e inferred from the ratio of opening displacement to load is preferable.

Measurements of $\mathcal{J}_c$ and K_c are useful primarily for situations in which the tangency point on the R-curve is unlikely to differ significantly from the plateau level of the R-curve. The ideal situation would be one in which the R-curve would rise steeply and turn abruptly onto its plateau. The behaviors of many materials correspond approximately to this ideal situation when the crack size and net section are larger than $2.5\ (K_c/\sigma_Y)^2$ as is required for ASTM evaluations of K_{Ic}.

In the preceding comments, we have inferred that calculations of $\mathcal{J}$ and K using the effective, or r_Y corrected, crack size retain characterization value even when r_Y is, say, half as large as the dimension, a, of the crack. That is to say, we have assumed the values of $\mathcal{J}$ and K, thus calculated, continue to serve as useful measures of the tendency toward onset of rapid fracturing even when the net section stress is nearly large enough for general yielding. A justification for this can be furnished in terms of the fact that a nearly constant proportionality of the plasticity corrected $\mathcal{J}$ to the crack opening stretch is retained throughout this stress range. Additional comments on this point will be provided in other lectures.

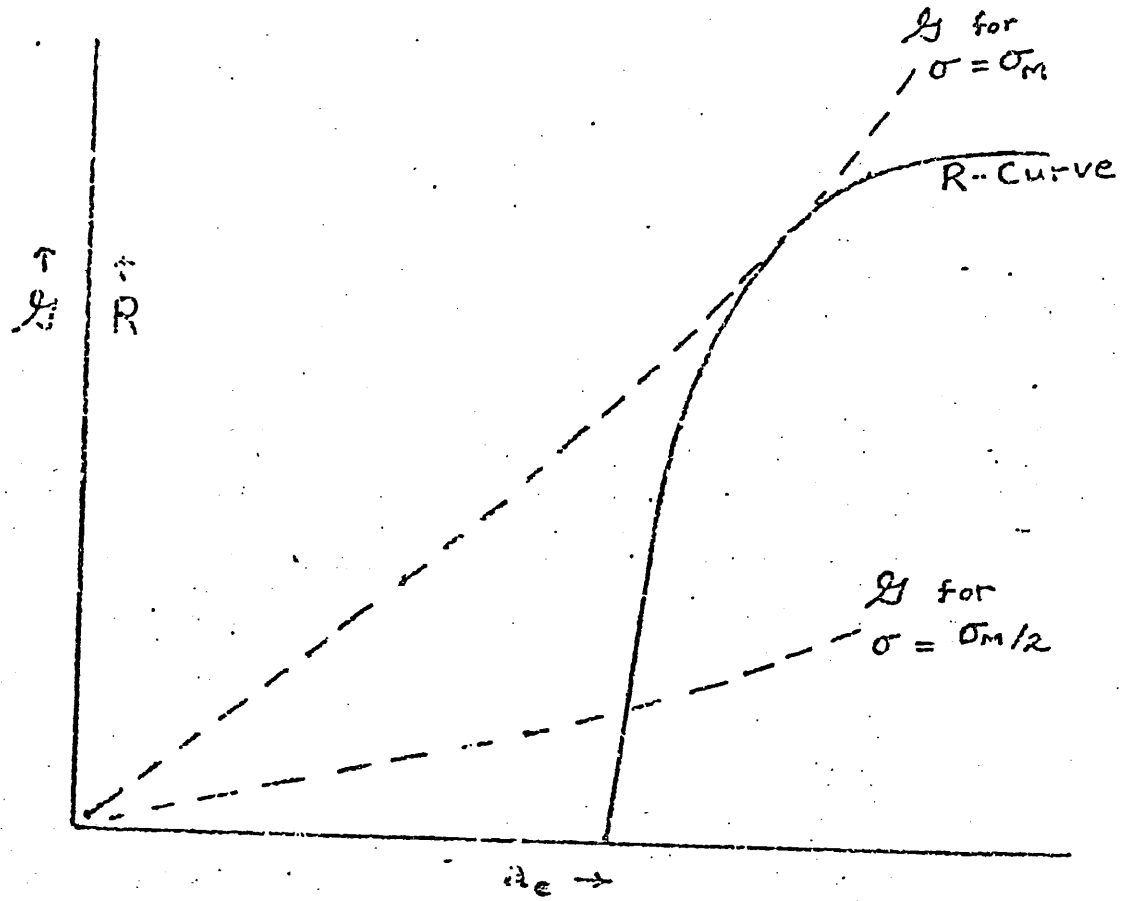

Figure 1 - R as a function of a_e for a typical high strength metal sheet material.

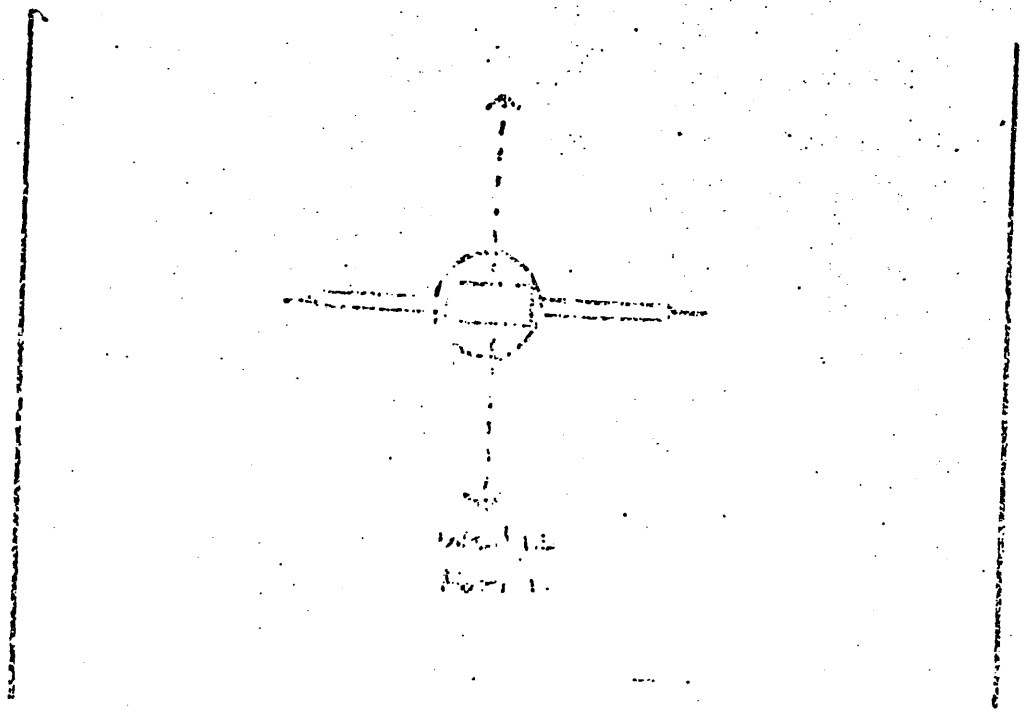

Figure 2 - Centrally located crack specimen noted in

REFERENCES

(1) ASTM Bulletin, January 1960 "Fracture Testing of High Strength Sheet Materials. Figure 9.

(2) J. M. Krafft, H. M. Sullivan, and R. M. Boyle, "Effect of Dimensions on Fast Fracture Instability of Notched Sheets", Proc. of Crack Prop. Symp. College of Aeronautics, Cranfield, England, Vol. I, pp. 8-26, (1961)

(3) C. M. Carman, D. F. Armiento, and H. Markus, "Crack Resistance Properties of High Strength Aluminum Alloys", Proc. of Int. Conf. on Fracture, Sendai, Japan, Vol. 2, pp. 995-1038, (1965)

(4) H. R. Heyer and J. E. McCabe, "Plane-Stress Fracture Toughness Testing Using a Crack-Line-Loaded Specimen" (To be published in Journal Engineering Fracture Mechanics) Vol. 3 ~1970

See R-Curve Measurement Method Book of ASTM Standards Vol. 10

ASTM Method

Fracture Toughness Measurements

From previous discussion, measurements of the resistance to crack extension as a function of effective crack size (R-curves) are assisted by two factors: (1) Use of wedge loading to postpone onset of rapid fracturing and use of large enough lateral dimensions so that the maximum K_R can be measured prior to yielding of the specimen. Because of the fact that the lateral dimensions are often large relative to the plate thickness, arrangements for R-curve testing should include fixtures which prevent out-of-plane deformation of the test plate. A compact tension specimen shape is suitable with the loading positions shifted to near the line of the crack simulating notch and revised to accommodate loading by a wedge displacement method. Since there is no direct record of the load applied by the wedges, crack opening displacements are recorded at two widely separated points.

A simplified version of R-curve testing can be done using a center-notched tension specimen. Lubricated plates to prevent out-of-plane deformation near the crack line can be held against the test plate using moderate clamping pressure. After calibration, a single measurement of crack opening displacement across the center of the crack simulating notch provides an estimate of the effective crack size during loading.

Although onset of rapid fracturing occurs prior to achievement of an upper plateau value of K_R, the portion of the R-curve provided by this test method can be extended by use of a displacement control loading method and may be adequate for practical applications, particularly if the test plate is relatively large.

The R-curve method for characterization of fracture toughness is of basic reference value in the case of K_c and K_{Ic} testing.

K_c Testing

Methods for K_c testing of high strength sheet materials were discussed in the ASTM Bulletin, January 1960. For best accuracy of this work, the testing arrangements do not differ significantly from those which would be used to make simplified R-curve determinations. An appropriate specimen design is one in which the crack simulating notch, including segments of fatigue cracking, has a total length of about one-third of the specimen width. A specimen length of twice the plate width between the loading reinforcement plates is desirable. K_c test results obtained with the net section stress less than 0.8 σ_{YS} generally do not differ significantly from the maximum value of K_R.

Static and dynamic measurements of K_c for structural steels have been performed using a 3-point loaded bend specimen with the crack simulating notch extending to 0.3 W. In this case W is the depth of the bend specimen. The principal simplification in fracture testing of relatively low cost structural steels is the absence of appreciable slow-stable cracking prior to onset of rapid fracturing. For slow loading measurements, determination of effective crack size can be assisted by use of a crack "mouth" opening displacement measurement. This is impractical in dynamic testing. However, the maximum load of the test can be obtained either from instrumentation on the specimen or from instrumentation on the striking tup. In the latter case, the load application should be "cushioned" so that the loading time is about 1 millisecond. Only a formal r_y type adjustment to obtain effective crack size is feasible in dynamic (impact) K_c fracture testing.

Although K_c testing methods have not yet received standardization treatment, such tests have been quite useful. Currently there is a considerable interest in the development of relationships between relatively simple impact

fracture tests (for example, Charpy-V-Notch tests) and tests which can be analyzed using fracture mechanics. Except for very low amounts of fracture toughness, the Charpy test appears to be too small to permit more than an empirical comparison. In the case of dynamic-tear tests, if the specimen indentation energy is taken into account, there is an understandable comparison between the values of $\mathcal{J}_c$ (when measurable) and the total fracture work per unit area.

With regard to the dimensional requirements for the centrally notched specimens, an approximate rule is that a close approach to general yielding occurs when $2r_Y = 1/2\ (\frac{W}{2} - a)$. In the case of the notched-bend specimen, the corresponding equation is

$$2r_Y = \frac{1}{4}\ (W-a)$$

K_{Ic} Testing

ASTM test method E-399 gives a complete and detailed description of K_{Ic} testing. The stringent requirements for test validity which one finds in test method E-399 resulted, in part, from the idea that the K_{Ic} value for any metal (of large enough section size) is of special fundamental importance and can be determined without allowance for R-curve influences such as the plastic zone and slow-stable cracking.

In its present form the test method depends rather critically upon a good determination of load as a function of crack "mouth" opening displacement. A line is drawn on the test record having a slope 5 percent less than the slope of a tangent to the initial portion of the test record as shown in Figure 1.

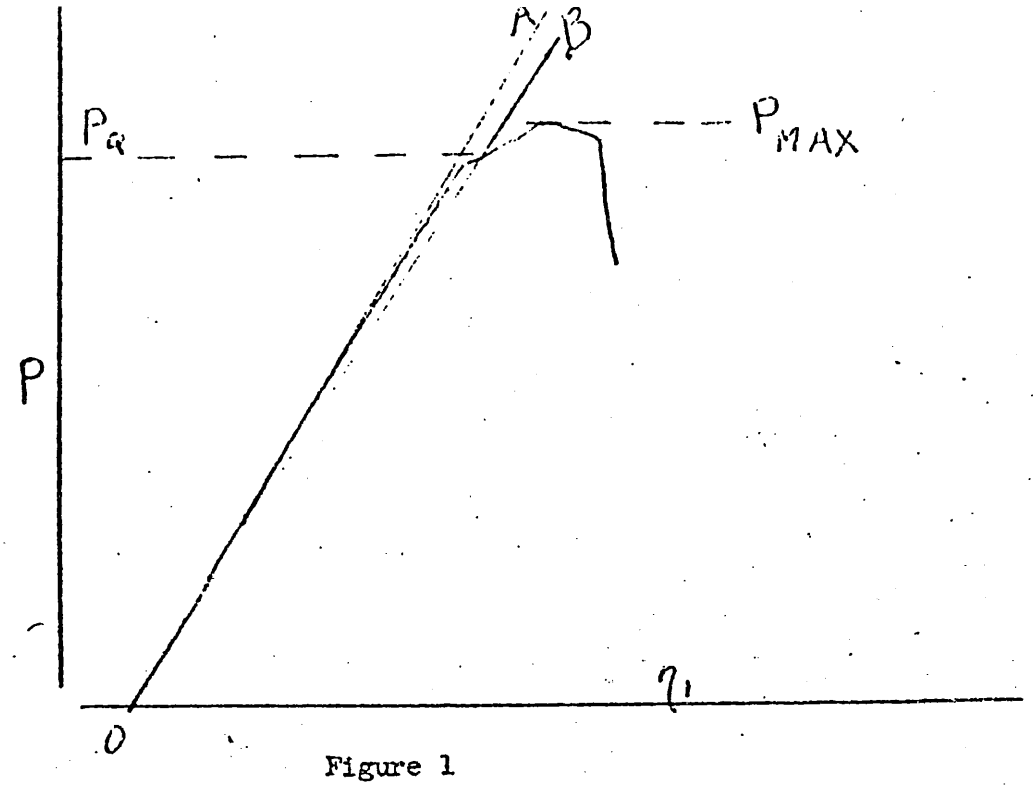

Figure 1

The highest point of the load-displacement line between OA and OB is the load, P_Q, used to calculate a K value for the test. The crack size used for this calculation is measured on the specimen after fracture and is the average of the center and quarter points of the sharp crack front established by low-amplitude fatigue cracking. The forward measurement position of any two points on the leading edge of the crack should differ by less than 10 percent of the crack size.

The principal dimension requirements are examined after calculation of a tentative estimate of K_{Ic} termed K_Q. It is necessary that the specimen thickness, B, the crack size, a, and the net ligament, W-a, are all greater than 2.5 $(K_Q/\sigma_{YS})^2$. An additional, after the fact, check is a comparison of the K_{MAX} used during the last segment of fatigue cracking to the value of K_Q the test method requires K_{MAX} (during final fatigue cracking) to be 0.6 K_Q or less.

The final validity requirement of the test method concerns the appearance of the testing record beyond the point, P_Q. If the test record shows a

load maximum beyond P_Q, the magnitude of this load maximum must not exceed P_Q by more than ten percent.

Equations for K

Center-notched-tension

$$K = \sigma \sqrt{\pi a} \left(\sec \frac{\pi a}{W}\right)^{1/2}$$

Notched-Bend Specimen

3 pt. loading $S/W = 4$

$$K = \frac{PS}{BW^{3/2}} \left(\frac{a}{W}\right)^{1/2} \left\{2.90 - 4.60\left(\frac{a}{W}\right) + 21.8\left(\frac{a}{W}\right)^2 - 37.6\left(\frac{a}{W}\right)^3 + 38.7\left(\frac{a}{W}\right)^4\right\}$$

Compact-Tension Specimen

$$K = \frac{P}{BW^{1/2}} \left(\frac{a}{W}\right)^{1/2} \left\{29.6 - 185.5\left(\frac{a}{W}\right) + 655.7\left(\frac{a}{W}\right)^2 - 1017.0\left(\frac{a}{W}\right)^3 + 638.9\left(\frac{a}{W}\right)^4\right\}$$

Fatigue Cracking

Most of us have had the experience of breaking an iron wire by repeated localized bending. Reversals of large plastic strains produce, at first, very small cracks and subsequently a joining of these. The formation of one or more cracks of substantial size relative to the wire diameter results in an easily detected loss of bending resistance and continued bending soon produces a complete separation. A similar process occurs at the leading edge of a crack when the crack is subjected to cycles of tension. At peak load of the first half-cycle, a zone of plastic strain of nominal size $2r_Y$ has

$$2\,r_Y = \frac{1}{\pi}\left(\frac{K_{MAX}}{\sigma_Y}\right)^2 \qquad (1)$$

formed resulting in very large plastic tensile strains adjacent to the crack tip. The unloading cycle can be regarded as a superimposed compression. In terms of stress intensity the magnitude of this added compression is $\Delta K = K_{MAX} - K_{MIN}$. The nominal size of the zone of plastic strain reversal is smaller than the initial (tensile) plastic zone because a compressive strain of $2\,\epsilon_Y$ is necessary to change the state of strain from one of tensile yielding to one of compressive yielding. The nominal plastic zone size computation can be adjusted for this by replacing σ_Y by $2\sigma_Y$ in the equation for $2r_Y$. In addition the magnitude of the added compression, ΔK, may be smaller than K_{MAX}. The result is an estimate of the reversed plastic strain zone size given by

$$(2r_Y)_{rev.} = \frac{1}{4\pi}\left(\frac{\Delta K}{\sigma_Y}\right)^2 \qquad (2)$$

Since the size of the zone of reversed plastic strains depends only upon ΔK and σ_Y, one might expect the fatigue crack growth rate, for a given structural metal, would depend primarily on ΔK. Experiments, in fact, show that

ΔK is the dominant factor controlling the crack growth rate per cycle, da/dN. Elevation of the mean K, K_{MAX} minus 1/2 (ΔK), adds only moderately to the observed da/dN value.

The limitations of linear-elastic analysis methods in applications to investigations of fatigue cracking tend to be less than those associated with fracture toughness measurements because the nominal plastic zone, particularly the reversal plastic zone size, tends to be smaller in the case of fatigue cracking. Furthermore, predictions of safe life in service can be made in a realistic manner because it is possible to take into account the influence of the initial defects which serve effectively as small starting cracks capable of enlargement by fatigue loading.

Fatigue cracking has often occurred in aircraft structures. Studies of fatigue crack growth rate, da/dN, as a function of ΔK for materials used in aircraft were introduced by P. C. Paris and his associates at the Boeing Company (Seattle) in 1957 and have received increasing attention during subsequent years. A typical graph of log (da/dN) versus log (ΔK) for a structural metal is shown in Figure 1.

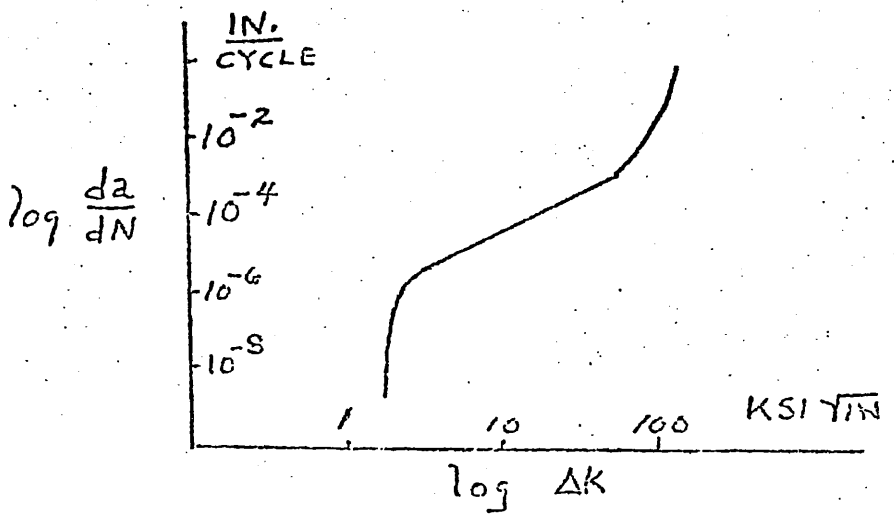

Figure 1. Typical behavior of da/dN as a function of ΔK

(The ordinate scale should be shifted upward by about a factor of 10)

Threshhold values of ΔK below which (da/dN) appears to be zero occur across the range of 1 to 15 KSI$\sqrt{IN}$ for various structural metals depending upon the mean K and testing temperature. Influences of the testing environment near the lower threshhold of ΔK must be regarded as uncertain for two reasons. (1) The experimental work confirming existence of these ΔK limits for fatigue crack growth has received publication and discussion only since 1970 (P. C. Paris, et al, at Del Research Corporation). (2) Of necessity for efficient collection of data most of this work has been done with high frequency loadings which tend to suppress influences of environment.

The rapid decrease of da/dN with decrease of ΔK has seemed to start in the range of da/dN values between 10^{-7} in/cycle and 10^{-8} in/cycle. At the right side of the behavior graph, in the range of da/dN values between 10^{-4} in/cycle and 10^{-3} in/cycle, a rapid increase of da/dN with ΔK is observed. As in the case of the lower threshhold region, additional experimental data is needed for clarification. With the present data, it is difficult to say whether the significant factor is the development of da/dN values larger than the spacing of fine scale inhomogeneities (for instance, grain size) or whether the significant factor is the approach of K_{MAX} toward the K_c value for the test plate.

The region which has received most study is the range of da/dN values between 10^{-7} in/cycle and 10^{-4} in/cycle. For this range, graphs of log da/dN versus log ($\Delta K/E$) for steels and alloys of Aluminum, Magnesium, and Titanium (with effects of environment suppressed) fall into an overlapping band, suggesting that fatigue cracking is primarily a kinematic process governed by the magnitude of plastic strain reversal at the crack tip.

An empirical equation of the form

$$\frac{da}{dN} = C\,(\Delta K)^n \qquad (3)$$

can be used to represent this region where C and n are empirical constants and n lies in the range of 2 to 4. Values of n larger than 3 usually indicate presence of some environmental influence. In any case, the development of appropriate values of C and n for the material and environment of interest furnishes a basis for predicting the fatigue life of a structure containing an initial crack-like flaw of given size.

For example, assure the expected loadings can be regarded as equivalent to application of a remote stress fluctuation, $\Delta\sigma$, where

$$\Delta\sigma = \sigma_{MAX} - \sigma_{MIN} \qquad (4)$$

Assume next that the starting crack is like a half-circle part-through crack at one surfaceof the component. The correction for the free surface will then be small (say 5 percent) and the ΔK at the leading edge of the crack is given approximately by

$$\Delta K = q\sqrt{a} \qquad (5)$$

where

$$q = 1.05\,(2/\pi)(\Delta\sigma)\sqrt{\pi} \qquad (6)$$

and a is the radius of the half-circle starting crack. From equations (3) and (5), and treating q as a fixed constant,

$$N = \int_{a_o}^{a_1} \frac{1}{c\,q^n}\,\frac{da}{a^{n/2}} \qquad (7)$$

$$N = \frac{a_o^{\,n/2}}{cq^n a_o\left(\frac{n}{2}-1\right)}\left\{1 - \left(\frac{a_o}{a_1}\right)^{\left(\frac{n}{2}-1\right)}\right\} \qquad (8)$$

The above integration assumes $n \geq 2$. One can readily see that, for situations of long life ($N > 10^5$ cycles), the initial da/dN value

$$\left(\frac{da}{dN}\right)_{initial} = c\,(q\sqrt{a_o})^n \qquad (9)$$

must be smaller than $a_o \times 10^{-5}$ (in/cycle). Furthermore, most of the life occurs with the crack size close to the value of a_o. In typical situations a_o may be in the range of 10^{-3} inches to 5×10^{-3} inches. Rapid completion of the fatigue crack through the plate or section thickness can be expected when a becomes as large as half of the section thickness, a dimension which is likely to be 100 times larger than a_o. Thus the second term in the curly brackets of equation (8) would not contribute significantly to the value of N.

It is a fortunate circumstance that most crack-like fabrication flaws are sufficiently blunted and irregular so that many cycles of loading are usually necessary in order to "sharpen" the leading edge and thus initiate fatigue cracking in correspondence to equation (3). In making judgments regarding the degree of perfection which must be established by process control and inspection, the extra fatigue life thus introduced cannot be given much weight if the service life is critical and must be guaranteed in a sure way. In the case of pressure vessels, a leak-before-burst toughness condition may provide a protective feature of importance through the fact that detection of leakage can be arranged to occur prior to onset of rapid fracturing. A comparable degree of fracture toughness in the case of other structural components may permit detection of fatigue cracks prior to onset of rapid fracturing if the inspections are sufficiently frequent. Otherwise fracture toughness plays a minor role in the case of N values larger than 10^5 cycles.

It is important to recognize that, for any given metallic material, fatigue cracking does not correlate with fracture toughness and yield strength when the N values of interest are large. In the case of low cycle fatigue ($N < 10^5$ cycles), the approach of the crack size to the value which is critical for onset of rapid fracturing may be quite important, particularly when the N value of interest is in the range of 10 to 500 cycles. For this range estimates of maximum amounts of fatigue crack extension can be made on the assumption that da/dN will be less than the cyclic range of the crack opening stretch, $\hat{\delta}$, where

$$\hat{\delta} = \frac{(\Delta K)^2}{2\sigma_Y E} \qquad (10)$$

With regard to random amplitude loadings, if an equation similar to equation (3) has been established for the material and the frequency of various $\Delta\sigma$ load fluctuations is known, current data suggests that use of average values of $(\Delta\sigma)^n$ results in conservative estimates of the crack growth rate. The reason for this is that the large $\Delta\sigma$ followed by smaller $\Delta\sigma$ values has a delaying influence on da/dN which is larger than the occasional da/dN increase introduced when a series of small $\Delta\sigma$ values is followed by several large values of $\Delta\sigma$.

Stress Corrosion Cracking

As in the case of fatigue cracking, studies of stress corrosion cracking are conducted at applied K values below K_c for the test plate and the adequacy of characterizations based upon linear-elastic analysis is rarely a significant consideration. On the other hand, the degree of plane-strain is of much greater significance in the case of stress corrosion cracking than in the case of fatigue cracking. Experimental graphs of da/dN versus ΔK have been developed extending through the region of change from flat-tensile into oblique-shear fracturing which show little apparent influence of this transition in fracture appearance. However, the development of moderate amounts of plane-stress plate thickness reduction near the crack tip has been observed to cause arrest of a crack extending under steady load with the aid of stress corrosion. For this reason studies of crack extension speed as a function of the applied K are usually conducted under condition of a plane-strain degree of constraint of the plastic zone. Thus the specimen thickness, crack size, and net ligament are generally about $2.5\ (K/\sigma_{YS})^2$, or more, across the range of K values subjected to investigation. Furthermore the degree of sensitivity to stress corrosion cracking tends to decrease with increase of K_{Ic} and decrease of σ_{YS}.

The term "stress-corrosion" used in this note can be regarded as equivalent to "agressive environment". The most common agressive environment is one which causes injection of hydrogen atoms into the structural metal. In the case of steels, roughly in order of severity, the following environments may cause deepening of a prior crack: air plus H_2O, pure H_2O, sea-water (water plus 3 percent NaCl), H_2 plus H_2O, water plus additives causing either a low pH or a high pH, pure H_2, gaseous H_2S. With environments of this nature, the crack speed depends upon the K value and the concentration of atomic hydrogen

in the fracture process zone. The hydrogen concentration in the fracture process zone depends upon the rate of injection of atomic hydrogen and upon the diffusion speed of the hydrogen atoms within the metal. As the speed of crack extension increases with increase of K, one frequently observes a behavior range within which additions to K cause little or no increase of crack speed. Studies of activation energy, Q, using the equation

$$\frac{da}{dt} = C\, e^{-\frac{Q}{RT}} \qquad (1)$$

have been conducted using observations of da/dt at a fixed K value as a function of the testing temperature, T, where T is the absolute temperature. When these studies were done with a K value large enough to produce the tendency toward a plateau in the crack speed versus K behavior graph, the resulting Q corresponded to the activation energy for diffusion of atomic hydrogen in the metal.

Figure (1) shows a schematic behavior graph of log (da/dt) as a function of the applied K value.

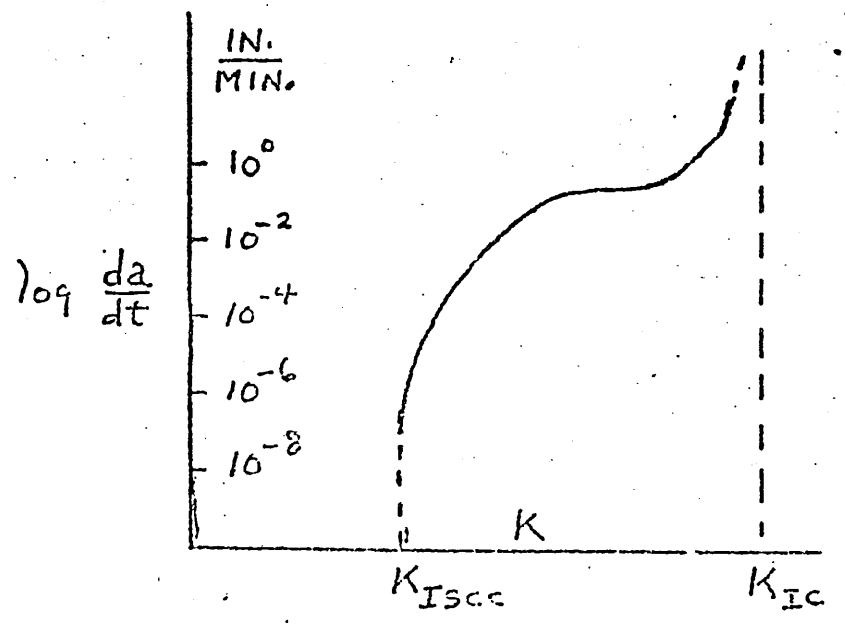

The K value termed K_{ISCC} is defined as the value of K above which a pronounced increase (toward values larger than 10^{-7} inches/minute) occurs in the crack speed with any significant increase of the K value. When crack speeds less than 10^{-7} inches/min. are of practical importance, and when the tendency toward a crack arrest threshhold is obscured by the influence of load fluctuations, these factors must be given study in experiments which tend to model the expected service conditions. Otherwise comparisons of K_{ISCC} values are of practical value in choosing materials of minimum sensitivity to stress corrosion cracking in the presence of crack-like fabrication flaws.

Measurements of K_{ISCC} can be done conveniently using specimens of compact tension shape but with the initial displacement fixed. The fixed load-displacement condition can be introduced in various ways. Possibly the simplest way is to use a bolt extending through the lower half of the specimen and exerting a pressure against the upper surface of the crack. If the loading line of the compact tension specimen is retained, one can use available calibration equations to obtain the relationship between load-displacement, crack size, and the K value. If the initial crack tip is sharpened by low amplitude fatigue and the initial opening displacement puts K above K_{ISCC}, then forward motion of the crack causes reduction of load and K value and crack arrest is observed at the K_{ISCC} value. After a long period of exposure to the environment, specimens in which crack motion appears to have stopped are removed from the environment, and subjected to an additional amount of fatigue cracking. The specimen is then broken at low temperature and examined to obtain a measurement of the stress corrosion crack depth at the arrest point. This crack depth along with the initial load-displacement permits calculation of the K_{ISCC} value for that specimen.

A recent interesting suggestion deserving further study has been made by investigators at the British Iron and Steel Institute Laboratory at Sheffield, England. The suggestion is that a few minutes of exposure of steel specimens to gaseous H_2S seems to produce the same K_{ISCC} value as obtained after six months of exposure of similar specimens to a water environment.

Standard K_{ISCC} measurement methods are currently under development by ASTM. It must be noted, however, that small amounts of stress corrosion assisted crack extension are likely to follow each appreciable load fluctuation even at values of K smaller than K_{ISCC}. Thus, if load fluctuations will occur in service, separate laboratory experiments which model these in a realistic manner are advisable. Furthermore, studies conducted using deep cracks are not influenced appreciably by the natural oxide coating of the metal. In order to obtain clarification and further understanding of the development of small surface cracks, for example cracks beneath corrosion pits, studies of cracking speed as a function of K using surface cracks of very small depth would be helpful.

F. M. Course notes prepared by G.R. Irwin,

COMPREHENSIVE FRACTURE CONTROL PLANS

For certain structures, which are similar in terms of design, fabrication method, and size, a relatively simple fracture control plan may be possible, based upon extensive past experience and a minimum adequate toughness criterion. It is to be noted that fracture control never depends solely upon maintaining a certain average toughness of the material. With the development of service experience, adjustments are usually made in the design, fabrication, inspection, and operating conditions. These adjustments tend to establish adequate fracture safety with a material quality which can be obtained reliably and without excessive cost. A fair statement of the basic philosophy of fracture control for such structures might be as follows. Given that the material possesses strength properties within the specified limits, and given that the fracture toughness lies above a certain minimum requirement (Nil-Ductility Temperature, Fracture Appearance Transition Temperature, Plane-Strain or Plane-Stress Crack Toughness), then it is assumed that past experience indicates well enough how to manage design, fabrication, and inspection so that fracture failures in service occur only in small tolerable numbers.

With the currently increasing use of new materials, new fabrication techniques, and novel designs of increased efficiency, the preceding simple fracture control philosophy has tended to become increasingly inadequate. The primary reason is the lack of suitable past experience and the increased cost of paying for this experience in terms of service fracture failures. Indeed, modern technology is beginning to exhibit situations with space vehicles, jumbo-jet commercial airplanes, and nuclear power plants for which not even one service fracture failure would be regarded as acceptable without consequences of disaster proportions. Consideration must be given, therefore, to comprehensive plans for fracture control such as one might need in order to provide assurance of zero service fracture failures. A review of the fracture control aspects of a comprehensive

plan may be advantageous even for applications such that the required degree of fracture control is moderate. One reason for this would be that an understanding of how to minimize manufacturing costs in a rational way is assisted when we assemble all of the elements which contribute to product quality and examine their relative effectiveness and cost. In the present case, the quality aspect of interest is the degree of safety from service fractures.

After these introductory comments, it is necessary to point out that the concept termed "comprehensive fracture control plan" is quite recent and cannot yet be supported with completely developed illustrations. We know in a general way how to establish plans for fracture control in advance of extensive service trials. However, until a number of "comprehensive fracture control plans" have been formulated and are available for study, detailed recommendations to guide the development of such plans for selected critical structures cannot be given.

The available illustrative examples of fracture control planning which might be helpful are those for which a large number of the elements contributing to fracture control are known. At least in terms of openly available information, these examples are incomplete in the sense that the fracture control elements require collection, re-examination with regard to relative efficiency, and careful study with regard to adequacy and optimization. Substantial amounts of information relative to fracture control are available in the case of heavy rotating components for large steam turbine generators, components of commercial jet airplanes (fuselage, wings, landing gear, certain control devices), thick-walled containment vessels for BW and PW cooled nuclear reactors, large diameter underground gas transmission pipelines, and pressure vessel components carried in space vehicles. Certain critical fracture control aspects of these illustrative examples are as follows.

A. Large Steam Turbine Generator Rotors and Turbine Fans

1. Vacuum de-gassing in the ladle to reduce and scatter inclusions and to eliminate hydrogen.
2. Careful ultra-sonic inspection of regions closest to center of rotation.
3. Enhanced plane-strain fracture toughness.

B. Jet Airplanes

1. Crack arrest design features of the fuselage.
2. Fracture toughness of metals used for beams and skin surfaces subjected to tension.
3. Strength tests of models.
4. Periodic re-inspection.

C. Nuclear Reactor Containment Vessels

1. Quality uniformity of vacuum degassed steel.
2. Careful inspection and control of welding.
3. Uniformity of stainless cladding.
4. Proof testing.
5. Investigations of low cycle fatigue crack growth at nozzle corners and of cracking hazard from thermal shock.

D. Gas Transmission Pipelines

1. Adequate toughness to prevent long running cracks.
2. High-stress-level, in-place, hydrotesting.
3. Corrosion protection.

E. Spacecraft Pressure Vessels

1. Surface finishing of welds so as to enhance visibility of flaws.
2. Heat treatment to remove residual stress and produce adequate toughness within given limits of strength.

3. Adjustment of hydrotesting to assure adequate life relative to stable crack growth in service.

In a large manufacturing facility, the inter-group cooperation necessary to achieve successful fracture control on the basis of a comprehensive fracture control plan may require special attention. In general, the comprehensive plan will contain various elements pertaining to Design, Materials, Fabrication, Inspection, and Service Operation. These elements should be directly or indirectly related to fracture testing information. However, the coordination of the entire plan to insure its effectiveness is not apriori a simple task. The following outline lists certain fracture control tasks under functional headings which might, in some organizations, imply separate divisions or departments.

I. Design

A. Stress distribution information.

B. Flaw tolerance of regions of largest fracture hazard due to stress.

C. Estimates of stable crack growth for typical periods of service.

D. Recommendation of safe operating conditions for specified intervals between inspection.

II. Materials

A. Strength properties and fracture properties.

σ_{YS}, σ_{UTS}, K_{Ic}, K_c.

K_{ISCC} for selected environments.

$\frac{da}{dN}$ for selected levels of ΔK and environments.

B. Recommended heat treatments.

C. Recommended welding methods.

III. Fabrication

A. Inspections prior to final fabrication.

B. Inspections based upon fabrication control.

C. Control of residual stress, grain coarsening, grain direction.

D. Development or protection of suitable strength and fracture properties.

E. Maintain fabrication records.

IV. Inspection

A. Inspections prior to final fabrication.

B. Inspections based upon fabrication control.

C. Direct inspection for defects using appropriate NDT techniques.

D. Proof testing.

E. Estimates of largest crack-like defect sizes.

V. Operations

A. Control of stress level and stress fluctuations in service.

B. Maintain corrosion protection.

C. Periodic in-service inspections.

From the above outline, one can see that efficient operation of a comprehensive fracture control plan requires a large amount of inter-group coordination. If a complete avoidance of fracture failure is the goal of the plan, this goal cannot be assured if the elements of the fracture control plan are supplied by different divisions or groups in a voluntary or independent way. It would appear suitable to establish a special fracture control group for coordination purposes. Such a group might be expected to develop and operate checking procedures for the purpose of assuring that all elements of the plan are conducted in a way suitable for their purpose. Other tasks might be to study and improve the fracture control plan and to supply suitable justifications, where necessary, of the adequacy of the plan.

FRACTURE CONCEPTS

1. PROGRESSIVE CRACK EXTENSION

Progressive forward motion of the leading edge of a crack occurs when the stresses, deformations, and advance openings reach critical conditions relative to local fracturing. Development and joining of advance openings is the mechanism of local fracturing usually observed. Because of the stress intensification near the leading edge of the crack, a gross section tensile stress below that necessary for general yielding may be large enough to cause forward motion of the crack.

2. FRACTURE PROCESS ZONE

Adjacent to the leading edge of the crack lies a region which contains the advance separations and the deformations directly associated with local separational mechanisms. This region is termed the fracture process zone. The size of the fracture process zone is about 5(COS) or less, where COS is defined later. (Concept 5a) Outside of a boundary line enclosing the fracture process zone, it is convenient to assume that the rules of continuum mechanics apply in a straightforward manner.

3. THE CRACK-EXTENSION FORCE, $\mathcal{G}$

The crack-extension force, $\mathcal{G}$, is defined as the system-isolated loss of stress field energy per unit of new separational area. The increment of new separational area is regarded as infinitesimal and virtual. Thus the ability to calculate $\mathcal{G}$ for a crack in a stress field does not imply actual forward motion of the crack.

4. COMPLIANCE BASED DETERMINATIONS OF $\mathcal{G}$

Assume that a plate-type test specimen of thickness, B, containing a through-the-thickness crack, is loaded by a force, P, and that displacement of the force application region (parallel to the force) is represented by the symbol, ℓ. Assume the region of application of the reaction force is stationary. Let U_T be the total stress field energy and assume the stress field energy is zero when P is zero. From the definition of $\mathcal{G}$,

$$\mathcal{G} = -\frac{\partial U_T}{B\,\partial a} \quad (\ell \text{ fixed})$$

where a is the crack length and B da is the increment of new (virtual) separational area. The system-isolated (fixed ℓ) requirement can be removed by correcting for the increase of stress field energy due to any movement, dℓ, of P. The equation for $\mathcal{G}$ then becomes

$$\mathcal{G} = -\frac{1}{B}\left(\frac{d\,U_T}{da} - P\,\frac{d\ell}{da}\right)$$

In the case of negligible non-linear effects, the compliance, C, is given by $\ell = CP$, and U_T is given by $U_T = P\ell/2$. It follows that

$$\mathcal{G} = \frac{P^2}{2B}\,\frac{dC}{da}$$

Measurements of C as a function of a can be used to determine (dC/da) as a function of a. Such measurements provide a compliance calibration of the test specimen, permitting determinations of $\mathcal{G}$ for various crack sizes using observations of parameter pairs such as P,a; P, ℓ; P, C; ℓ,C.

5. FAST-STABLE CRACK EXTENSION

The fracture process zone of a running crack exhibits a low-inertia, overdamped type of behavior. At velocities between the upper limiting speed and crack arrest, the forward velocity of the process is closely controlled by the driving force, $\mathcal{G}$.

(a) Limiting Velocity

From purely inertial considerations, the velocity of a crack cannot be larger than the speed of Raleigh waves, about $0.9c_2$. ($c_2 = \sqrt{\mu/\rho}$, where μ is the rigidity modulus and ρ is the density). In real solids, the upper limiting velocity varies inversely with separational energy dissipation. Observed limiting speeds for fast-stable cracking have been in the range of $0.1c_2$ to $0.6\ c_2$.

(b) Crack Division

Increase of $\mathcal{G}$ beyond the amount necessary to drive a crack at limiting speed results eventually in crack division. For a deeply embedded crack in a

brittle solid, the efforts at crack division are locally independent along various segments of the leading edge so that crack division produces a very rough fracture appearance termed "hackle".

(c) Crack Arrest

The decrease of crack speed with decrease of $\mathcal{G}$ is terminated by crack arrest. Crack arrest is a relatively abrupt decrease of the crack velocity to zero (or nearly to zero).

(d) Onset of Rapid Fracturing

The opposite behavior to crack arrest is the relatively abrupt increase of crack speed which often occurs at the beginning of crack extension from the leading edge of a stationary crack or of a crack simulating notch. The degree of abruptness and the initial velocity increase with notch root radius (for a notch) or with leading edge roughness (for an initial crack).

6. SLOW-STABLE CRACK EXTENSION

At values of $\mathcal{G}$ too small for onset of rapid fracturing, stable progressive crack extension can occur due to stress corrosion, fatigue, viscosity, and unnatural sharpness of the initial crack. Slow-stable cracking due to sharpness of the initial crack is a portion of the resistance curve (R-curve) concept discussed later.

(a) Stress Corrosion Cracking

Because of lack of better terminology, all mechanisms of slow-stable cracking due to an agressive environment are commonly termed stress corrosion cracking. Hydrogen, either injected by electro-chemical action or already present in a metal, is attracted to the fracture process zone by the reduced density of that region and is often the agressive agent. In the case of mica, the influence of H_2O appears to be mainly one of reducing electric bonding forces between the crack surfaces. Such processes tend to be slow-stable because of the limited

diffusion rate of the active agent. With increase of $\mathcal{K}$, a crack speed "plateau" (where crack speed is insensitive to $\mathcal{K}$) is often observed. In the case of metals, frequent efforts at crack division are characteristic. With decrease of $\mathcal{K}$, an arrest point of corrosion cracking can often be observed.

(b) Fatigue cracking

When the leading edge of a crack is subjected to cycles of tensile loading, the large strain reversals at the leading edge of the crack result in increments of forward motion of the leading edge. The cyclic rate of crack extension, da/dN, is mainly a function of the cyclic range of the $\mathcal{K}$ value, $\Delta\mathcal{K}$. At values of da/dN below 10^{-7} inches per cycle, careful experiments reveal an abrupt decrease of da/dN toward zero with further decrease of $\Delta\mathcal{K}$.

(c) Viscous Cracking

In the case of polymeric solids composed of linear molecules, viscous stretch accompanied by molecular orientation and voids near the leading edge of a crack provide a mechanism for slow-stable crack extension prior to onset of rapid fracturing. The process speed increases and decreases in phase with slow continuous changes of $\mathcal{K}$. Slow stable cracking with similar characteristics has been observed in certain glasses and metals.

7. CRACK STRESS FIELD MODES

From two-dimensional linear-elastic analysis, the stress field close to the leading edge of a crack can be divided into three modes. Assume Cartesian coordinates with y normal to the plane of the crack, z parallel to the leading edge, and x directly forward coplanar with the crack. Mode I: τ_{xy} and τ_{yz} are zero on $y = 0$. Mode II: σ_y and τ_{yz} are zero on $y = 0$. Mode III: σ_y and τ_{xy} are zero on $y = 0$. For nearly isotropic materials, progressive tensile cracking occurs only with a Mode I stress field around the leading edge of the crack. The three stress field modes are only defined in a strict sense assuming plane-strain for Modes I and II and anti-plane strain for Mode III.

8. THE STRESS INTENSITY FACTOR, K.

In addition to the Carterian coordinates noted above, assume cylindrical coordinates, r, θ, z around the leading edge with z coincident with the leading edge and θ measured from the x axis. From linear-elastic stress analysis, assuming an isotropic solid, the stresses very close to the leading edge for a Mode I stress field are given by

$$\left.\begin{matrix}\sigma_y \\ \sigma_x \\ \tau_{xy}\end{matrix}\right\} = \frac{K \cos\frac{\theta}{2}}{\sqrt{2\pi r}} \left\{\begin{matrix}1 + \sin\,\theta/2 \sin 3\,\theta/2 \\ 1 - \sin\,\theta/2 \sin 3\,\theta/2 \\ \sin\,\theta/2 \cos 3\,\theta/2\end{matrix}\right.$$

To achieve extended usefulness in the case of orthotropic materials and fast stable cracks, the K value for Mode I is defined as

$$K = \text{Limit } (\sigma_y \sqrt{2\pi r})$$
$$\text{as } r \to 0 \text{ on } \theta = 0$$

Similar definitions are obtained for the Mode II and Mode III K values if σ_y is replaced in the above equation by τ_{xy} and τ_{yz} respectively.

9. RELATION OF K^2 to G.

For the tensile or opening mode (Mode I) cracks, which are of primary interest,

$$K^2 = E_1 \mathcal{G} \text{ where } E_1 = \begin{cases} E, & \text{plane-stress} \\ \dfrac{E}{1-\nu^2}, & \text{plane-strain} \end{cases}$$

E is Young's Modulus and ν is Poisson's ratio.

10. THE PLASTICITY ADJUSTMENT FACTOR, r_Y.

(a) Effective Crack Size

The characterization factors, K and G, computed from linear analysis can be given extended usefulness by increasing the "visual" or actual crack size so as to place the leading edge of the crack for analysis purposes at a central location within the crack tip plastic zone. This can be done in a conventional manner by advancing the position of the actual crack tip by the amount, r_Y, where

$$r_Y = \frac{1}{2\pi}\left(\frac{K}{\sigma_Y}\right)^2$$

Alternatively, when the load-displacement record for a test specimen shows curvature due to growth of a plastic zone (plus any slow-stable cracking), the crack size corresponding to the "apparent" compliance can be used as the effective crack size. σ_Y is an approximate estimate of the average y-direction tensile stress across the crack tip plastic zone.

(b) Nominal Plastic Zone Size

It is often useful to know whether the size of the plastic zone is large or small relatively to plate thickness or net ligament size. For such purposes $2\,r_Y$ can be regarded as a nominal measure of the plastic zone size.

11. PLANE-STRESS AND PLANE-STRAIN

Consult standard reference books on elasticity for definitions of plane-strain, generalized plane-strain, plane-stress, and generalized plane-stress.

(a) For a through-crack in a plate with in-plane loading, computations of K are customarily based on two dimensional analyses. The values of K and of $\mathcal{G}$ (plane-stress) thus obtained provide characterizations applicable to the leading edge region of the crack on a thickness average basis. When $2\,r_Y$ is small compared to the plate thickness, the leading edge stress field in the central portion of the plate thickness ~~may be~~ is nearly plane-strain. Methods of three-dimensional analysis suitable for accurate computation of K and $\mathcal{G}$ for this central region are not available. However, it is plausible to assume that the central region $\mathcal{G}$ value, if computed, would not differ significantly from the thickness-average value of $\mathcal{G}$ furnished by the two-dimensional plane-stress analysis. Although it is sometimes appropriate to regard plane-strain conditions as controlling onset of rapid fracturing in a plate-type test specimen, the region of plane-strain is relatively small. In specimens of the above type, regardless of the plastic zone size, the appropriate viewpoint for analysis of stresses and displacements away from the leading edge of the crack is generalized plane-stress.

(b) The appropriate value of σ_Y for use in computations of r_Y is a judgment choice. As a matter of terminology, assume

$$r_{YS} = \frac{1}{2\pi}\left(\frac{K}{\sigma_{YS}}\right)^2$$

where σ_{YS} is the uni-axial tensile yield point. For $2r_{YS} > \frac{2B}{3}$, the degree of plane-strain is small and choice of σ_Y as equal to σ_{YS} usually provides sufficient accuracy. However, choice of σ_Y as the average of σ_{YS} and the ultimate tensile strength, σ_{TS}, is often preferred when both are known. When $2\,r_{YS} < B/3$, the degree of plane-strain is substantial and the preferred estimates of σ_Y are elevated above the large plastic zone choice by a factor in the range of $\sqrt{3}$ to 2. When $\frac{2B}{3} > 2r_{YS}\ B/3$, an intermediate estimate of σ_Y is appropriate. The uncertainties in choice of σ_Y are relatively unimportant in practical applications.

(c) From linear-elastic treatment of three-dimensional crack problems, such as the flat elliptical or flat circular crack in a large solid, the stress equations ~~of small leading edge segments of these cracks~~ correspond exactly to generalized plane-strain only in the limit of infinitesimal closeness to the leading edge.

12. FRACTURE TOUGHNESS

(a) Resistance Curves (R-Curves)

When the "sharpness" of an initial crack is enhanced by a segment of low amplitude fatigue cracking, the initial increments of crack extension during a rising load test tend to be stable because the resistance to crack extension increases rapidly with the development of natural roughening of the leading edge. When the fracture toughness is large enough so that shear lips of substantial size develop, the period of stable crack growth is extended and it is usually possible to make a graphical plot of $\mathcal{G}$ (or K) as a function of actual (or effective) crack size prior to onset of rapid fracturing. The ordinate values are termed $\mathcal{G}_R$ or K_R) and such a graph is termed an R-curve. In the case of strain rate insensitive materials (aluminum alloys, ultra-high strength steels) and when onset of rapid fracturing is suppressed by use of wedge loading, it can be demonstrated that $\mathcal{G}_R$ and K

approach maximum values. The R-curve concept is fundamental to other forms of fracture toughness evaluation.

For strain rate sensitive materials (steels with $\sigma_{YS} < 160$ KSI), the abrupt fine scale separations inherent to natural fracturing introduce dynamic loading effects which frequently cause onset of rapid fracturing after a relatively short segment of crack extension. For dynamic testing of such materials, although direct R-curve measurements are not feasible, it is useful to think of the fracture energy in a dynamic-tear test as the area under a dynamic R-curve plotted in terms of $\mathcal{G}_R$.

(b) Plane-Strain Fracture Toughness

When the thickness of a plate type specimen is increased enough so that $B \geq 2.5\ (K/\sigma_{YS})^2$ at onset of rapid fracturing, the degree of plane-strain constraint of the plastic zone is large and the thickness average value of $\mathcal{G}$ at onset of rapid fracture, termed $\mathcal{G}_{Ic}$, can be regarded as a measure of the plane-strain fracture toughness. An ASTM testing standard (E-399) has been developed for measurements of plane-strain fracture toughness. In the present form of this test method, the measure of plane-strain fracture toughness, K_{Ic}, is determined from the thickness average $\mathcal{G}$ using the equation, $K^2 = E\mathcal{G}$. In addition the measurement point is placed at approximately 2 percent increase in size of the initial crack unless onset of rapid fracturing occurs previously. Other details and various requirements for validity of a test result are stated in the ASTM test method.

(c) Plane-Stress Fracture Toughness

Computations of the plane-stress fracture toughness, K_c, are commonly made using the effective crack size and load at onset of rapid fracturing. The measurement point load is usually taken to be the maximum load. The effective crack size is either derived from "apparent" compliance or is the visual crack size plus r_Y. Although no firm testing standards have been developed, it is

preferable to use specimens which are large enough so that the net section stress is at least 20 percent below the stress level for general yielding.

(d) Fracture Toughness Transitions

When $1/4B < 2r_{YS} < 2B$, the fracture toughness changes inversely with the plate thickness because of the change in constraint of the crack tip plastic zone. When the degree of plane-strain constraint is large, the fracture surfaces are normal to the direction of largest tensile stress with an appearance which is often termed "flat-tensile". When $2r_{YS} > 2B$, although the direction of fracturing remains normal to the largest tensile stress, the fracture is usually tilted as if the separation preferred planes of maximum shear stress. A term often used for this fracture appearance is "oblique-shear".

In the case of steels and in certain other BCC metals, with sufficient lowering of the testing temperature, the nature of a flat-tensile fracture changes from fibrous to quasi-cleavage. A large increase in the plane-strain fracture toughness is observed as the test temperature is increased through the range of transition from quasi-cleavage to fibrous fracturing. This is a micro-structural transition which depends upon the magnitude of the tensile stress across the fracture process zone as well as upon microstructural aspects such as grain size. Quasi-cleavage fracturing can be suppressed by inadequate constraint. Thus the two kinds of fracture transition are not independent. Their combined effect often causes a sufficiently abrupt change in fracture toughness with temperature so that "service temperature above transition temperature" provides a useful rule for adequate fracture toughness.

(e) Empirical K_c, K_{Ic} Relationship

Define ρ_c and ρ_{Ic} by the equations

$$\rho_c = \frac{1}{B}\left(\frac{K_c}{\sigma_{YS}}\right)^2 \qquad \text{and} \qquad \rho_{Ic} = \frac{1}{B}\left(\frac{K_{Ic}}{\sigma_{YS}}\right)^2$$

For $\rho_c < 2\pi$, an approximate empirical relationship exists in the form

$$\rho_c = \rho_{Ic}\left(1 + 1.4\,\rho_{Ic}^2\right)$$

(f) Dynamic-Tear and Charpy V-N Notch Testing

A dynamic-tear (DT) test is a 3-point loaded notched-bend test broken by a falling weight or a pendulum impact. When the notch sharpness is adequate and energy dissipation at the loading points is negligible, the measured fracture energy can be regarded as the area under the dynamic R-curve (plotted in terms of $\mathcal{J}_R$).

Charpy-V notch (CVN) tests are similar except that the specimen is small (10 mm square cross section) and the notch root radius is 0.1 mm. Approximate empirical relationships have been suggested for computations of K_{Ic} (static) and K_{Ic} (dynamic) from CVN test results for structural steels.

13. Concepts of Adequate Toughness

Given a test specification which requires a substantial degree of toughness, for a given class of structures it is usually possible to adjust the design, fabrication, and inspection so that only a tolerable number of fracture failures are experienced.

(a) Leak-Before-Burst Concept

From the plasticity adjusted value of K for a through-crack of length, 2B, in a large plate with a tension, σ, normal to the crack, one can derive the equation

$$\beta_c = \frac{\pi y^2}{1-0.5y^2} \qquad \text{where } y = \sigma / \sigma_{YS}$$

Using the empirical K_c, K_{Ic} relationship, values of σ termed σ_{LB} can be derived from the above equation for given values of K_{Ic}, B, and σ_{YS}. This is regarded as the operating stress below which a short through-crack, if developed, will cause leakage of a pressure vessel prior to onset of rapid fracturing. A similar concept of adequate toughness has been suggested for other structures in which leakage is not a factor such as steel bridges.

(b) β'_{Ic} Equals Unity

A suggested simplification of the Leak-Before-Burst concept is $\beta_{Ic} = 1$. This concept has the virtue of requiring a fracture toughness which increases with yield strength and with section thickness.

(c) Requirements in Terms of DT and CVN

When a DT or CVN specimen of fixed dimensions is employed for the fracture toughness evaluations, the section thickness and σ_{YS} appropriate to a given structure must be separately taken into account, usually through empirical correlations. Full thickness DT specimens are particularly appropriate when arrest of a running crack is an important fracture control element.

14. FRACTURE CONTROL PLANS

A fracture control plan lists the plausible fracture hazards, discusses the relative efficiency of various methods for prevention of serious fractures, justifies estimates of safe loads and safe service lives, and assigns responsibility for each fracture control task. A complete fracture control plan involves inspection, fabrication, materials selection, and design in interdependent ways.

15. CHARACTERIZATIONS OF THE FRACTURE PROCESS ZONE

(a) Crack Opening Stretch, COS or δ

From several oversimplified elastic-plastic analyses of the crack tip region, the crack opening stretch near the leading edge of a crack is given by $\delta = \mathcal{J}/\sigma_Y$. The COS can be regarded as an average-strain type of characterization of the fracture process zone. Above general yielding, approximate estimates of COS can be made from slip line theory and from thickness reduction measurements.

(b) The J-Integral Concept

Assuming negligible crack motion, it can be shown that the stress-strain state around the fracture process zone can be approximately characterized by a path independent integral termed J. This concept permits determinations of J from calibration experiments. A series of crack lengths are used and J is derived as equal to $\mathcal{J}$

assuming the P, ℓ curves can be treated as if the material were non-linear elastic. There is no essential difference between J and the plasticity adjusted value of $\mathcal{J}$ below general yielding. It appears that a relationship of the type $J = \sigma_Y \delta$, holds both above and below general yielding.

ENERGY DISAPPEARANCE RATE, J, FOR A LINEAR (or NON-LINEAR) ELASTIC SOLID

A J-Integral contour around the crack tip fracture process zone might, for example, follow the elastic-plastic boundary (dashed) or the small circle, as shown in Figure 1.

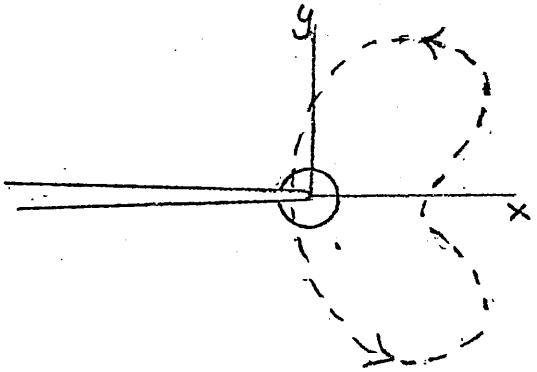

Figure 1

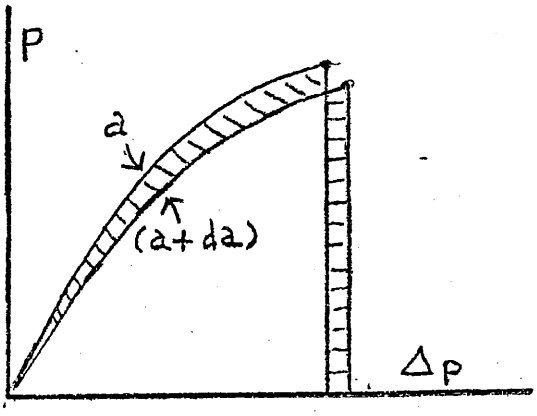

Figure 2

A general load versus load-displacement diagram for loading at a single (non-stationary) point is shown in Figure 2. Slant shading shows the energy disappearance, J da , for Δ_p fixed. Horizontal shading shows the recoverable stored elastic energy, P $d\Delta_p$, due to a small increase of load-displacement. If U_T is the total stored elastic energy,

$$J\,da = -dU_T + P\,d\Delta_p$$

Thus the definition of J, assumed here, does not differ from the definitio of $\mathcal{G}$. However, $\mathcal{G}$ has been closely associated with linear-elastic analysis and use of a new symbol for non-linear applications is not inappropriate.

We next take the viewpoint that the solid of interest is simply the area within an arbitrary selected contour which encloses the crack tip. Since energy loss during an increment of crack extension can take place only at the crack tip, a proper computation of the energy loss rate for the selected area must agree with a similar computation for the entire solid.

Along any segment, dS, of the J-Integral contour the applied load (corresponding to P) is the stress vector, $\vec{t}$, times dS. The load-displacement (corresponding to $d\Delta_p$) is $\frac{\partial \vec{u}}{\partial a} da$ where $\vec{u}$ is the displacement vector. We will indicate the product of load time parallel increment of load-displacement by a dot product convention and will write it as

$$\text{“}P\, d\Delta_P\text{”} = \left(\vec{t} \cdot \frac{\partial \vec{u}}{\partial a}\right) da\, dS$$

The total of the recoverable stored energy, corresponding to the horizontal shaded area of Figure 2, is given by a contour integral of all the boundary elements.

$$\Sigma \text{“}P\, d\Delta_P\text{”} = \oint da \left(\vec{t} \cdot \frac{\partial \vec{u}}{\partial a}\right) dS$$

Since

$$dU_T = \iint dx\, dy\, \frac{\partial U}{\partial a}\, da$$

where U is the stress field energy density, the expression for J can be written as

$$J = -\iint dx\, dy\, \frac{\partial U}{\partial a} + \oint \left(\vec{t} \cdot \frac{\partial \vec{u}}{\partial a}\right) dS$$

In comparing the above equation with the equation previously given for J da, it can be noted that the common factor, da, has been dropped from each of the three terms. The above equation can be simplified by recognizing that the crack size gradient terms, such as $\frac{\partial U}{\partial a}$, can be replaced by $-\frac{\partial U}{\partial x}$ etc. In other words, from the analysis viewpoint it is not possible to distinguish between an infinitesimal advance of the crack tip to the right and an infinitesimal shift of the coordinate origin to the left. When $-\frac{\partial U}{\partial x}$ is substituted for $\frac{\partial U}{\partial a}$ in the area integral, the integration with respect to x can be completed so that

$$J = \oint \left\{ U\, dy - \vec{t} \cdot \frac{\partial \vec{u}}{\partial x}\, dS \right\}$$

It can be shown that the above (Rice) form of the J-Integral is path independant if

$$\frac{\partial U}{\partial x} = \sigma_x \frac{\partial \varepsilon_x}{\partial x} + \sigma_y \frac{\partial \varepsilon_y}{\partial x} + \tau_{xy} \frac{\partial \gamma_{xy}}{\partial x}$$

The above equation is always true for elastic solids. When J is used for a solid with non-linear plastic behavior, U must be computed as if the behavior were non-linear elastic. More specific, U must be interpreted so that the above equation for $\frac{\partial U}{\partial x}$ remains valid.

If the behavior of the solid around (not within) the fracture process zone is described for analysis purposes in terms of deformation theory plasticity and the crack tip characterized moves only a small distance (relative to plastic zone size) during loading, J can be regarded as a path independent characterization of the stress-strain state around the fracture process zone. Numerical calculations which assume incremental plasticity behavior do not show a significant degree of path dependency of J. Use of J as a characterization parameter for fracture toughness measurements has permitted extension of such measurements to specimens in which considerable net section yielding occurs prior to the crack extension measurement point. Other applications of the J parameter are under development.

It should be noted that the equation referred to above as the Rice equation is not the basic definition of J. In special situations one must return to the basic idea of energy disappearance rate for an elastic solid. For example: (a) For rapid crack extension, the strain energy density, U, must be supplemented by terms which represent the kinetic energy density. (b) When there are body forces within the J-integral contour, their contribution to recoverable strain energy must be included in the J calculation. This is rather obvious for a crack in a rotating component. A less obvious varient occurs when a crack is in a stress field produced by a temperature gradient.

(c) When the stress field is 3-dimensional, except for special situations of axial symmetry, the J calculation must be restricted to the region near the crack front where the stress-strain field is nearly 2-dimensional. (d) In all of the above special situations, a proper calculation of J can be obtained by taking a limit of the J-integral, in the Rice form, as the dimensions of the contour approach zero. When this limiting procedure is used, any fixed shape of the contour can be selected arbitrarily.

For calculation purposes, it is often convenient to replace the vector (Rice) form of the J-integral equation by the following equivalent expression,

$$J = \oint \left\{ dy \left(U - \sigma_x \frac{\partial u}{\partial x} - \tau_{xy} \frac{\partial v}{\partial x} \right) + dx \left(\sigma_y \frac{\partial v}{\partial x} + \tau_{xy} \frac{\partial u}{\partial x} \right) \right\}$$